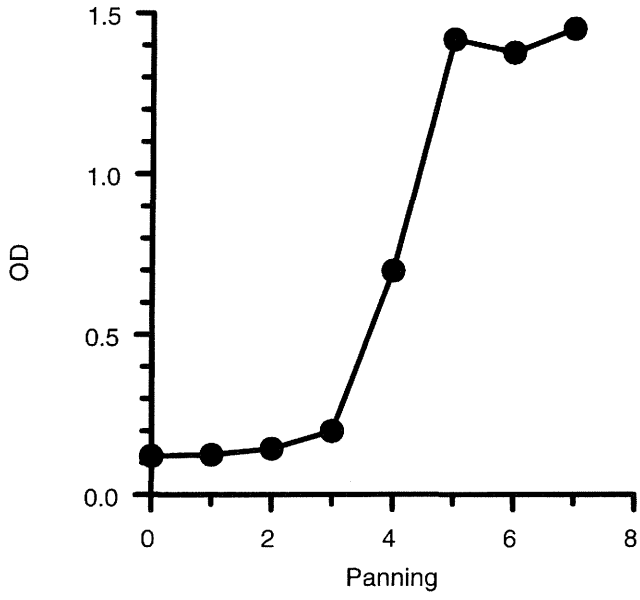

FIG. 3. Reactivity of phage to SIV Ag increased from the fourth round of panning. Phage samples that were eluted after panning were examined by ELISA for their ability to bind SIV proteins.

majority of these primer pairs worked with efficiency sufficient for the construction of the Ig library.

Construction of Fab library from SIVsmH635FC-infected macaque H723

The Fab library was constructed using the pComb3X system [37] from RNA extracted from lymph nodes of rhesus macaque H723, which was infected with a derivative of SIVsmE543-3, SIVsmH635FC.[31,32] This animal was used as a source of RNA since previous studies demonstrated that it mounted a vigorous antibody response.[31] Plasma collected at the time of death from H723 contained abundant antibodies against viral structural proteins Env and Gag (Fig. 2A). The NAb titer of plasma from this macaque sharply increased in acute infection and remained high until death (Fig. 2B), making this an attractive source of Ig genes for this study. The Ig variable regions, VH, Vκ, and Vλ, which were amplified from a lymph node of H723 (Fig. 1), were joined to conserved domains, CH1, Cκ, and Cλ, by overlap extension PCR, respectively. The final Fab gene fragment, which was generated by overlap extension PCR of heavy and light chains, was inserted into pComb3X after digestion with *Sfi*I. The resultant ligation mix was transformed into XL1-Blue *Escherichia coli* cells, and the phage library was prepared by adding helper phage. The size of the Ig library from macaque H723, estimated by the ability to transform XL1-blue, was 2.1×10^8 CFU.

Selection of SIV-specific Fab clones by panning

Biopanning was performed on a whole, Triton X-100-disrupted SIVsmE543-3 Ag-coated 96-well plate. The ability of phage to bind SIV Ag increased from the fourth round of panning, indicating successful selection of SIV-specific Fab (Fig. 3). Phagemid DNA was prepared from the fourth and fifth round of panning, and transformed into TOP10F′ *E. coli* cells to select clones that produce SIV-specific Fabs. Colonies were screened for reactivity of bacterial supernatants to SIV Ag using ELISA. SIV-specific Fab clones were sequenced, and a total of 20 independent clones were obtained (Table 2). Sequence analysis revealed that Fab clones expressed VH alleles, IGHV3 and IGHV4; Vκ alleles, IGKV1 and IGKV2; and Vλ

TABLE 2. CHARACTERISTICS OF FAB CLONES FROM AN SIV-INFECTED RHESUS MACAQUE

Clone	*VH allele*	*VH CDR3*	*Vκ or Vλ allele*	*Vκ or Vλ CDR3*	*WB*[a]	*NA*[b]
B404	IGHV3-h*01(P)[c]	TTGLQISEWFSTDGDEYFEF	IGLV3-25*02	QSSSGYHWV	gp120	>90%
B406	IGHV3-h*02(P)	VSGLQVSEWFSTDGDEYFEF	IGLV6-57*01	QSVDGTYNRL	gp120	>90%
B433	IGHV3-h*01(P)	SRGADFWSGSDRYFDF	IGLV3-25*02	HSVDSSAHHWV	gp120	>90%
B448	IGHV3-h*01(P)	TTGLQISEWFSADGDEFFEF	IGLV6-57*01	QSIDGYNRL	gp120	>90%
B402	IGHV4-4*07	IKQSYGRTV	IGKV2-40*01	MQGLDFPFT	gp41	—[d]
B405	IGHV4-28*01	ARRGGGPRARWFDV	IGKV2-40*01	MQALGFPPT	gp41	—
B407	IGHV4-4*07	ARRGVLRTSRIFDF	IGKV2-40*01	MQALGFPPT	gp41	—
B408	IGHV4-4*02	IKQSYGRTI	IGKV2-40*01	MQALQFPFT	gp41	—
B416	IGHV4-28*01	ARRGVYAGSRVFDF	IGKV2-40*01	MQAREFPPT	gp41	—
B417	IGHV4-4*02	VRRGVSAPAGTMLYFDL	IGKV2-40*01	MQGIESPPT	gp41	—
B418	IGHV4-4*07	IKQSYGRTI	IGKV2-40*01	MQGLDFPFT	gp41	—
B431	IGHV4-30-2*01	ARRGSYCSGNQCSRIFDS	IGKV2-40*01	MQALGFPPT	gp41	—
B434	IGHV4-4*02	VRRGVSAPAGTMLYFDL	IGKV2-40*01	MQGIESPPT	gp41	—
B438	IGHV4-28*05	ARRGVYAGSRVFDF	IGKV2-40*01	MQSLEFPPT	gp41	—
B442	IGHV4-28*01	ARRGVYAGSRVFDF	IGKV2-40*01	MQALGFPPT	gp41	—
B444	IGHV4-39*07	ARRGSICSGNQCSRIFDY	IGKV2-40*01	MQALGFPPT	gp41	—
B503	IGHV4-4*07	IKQSYGRTV	IGKV2-40*01	MQGLDFPFT	gp41	—
B505	IGHV4-b*01	ARRGVIGTSRIFDF	IGKV2-40*01	LQGLGFPPT	gp41	—
B450	IGHV4-39*07	ARQGPAAGVDS	IGKV1-17*01	LQHYSYPLT	p27	—
B455	IGHV4-4*07	ASHNFWSGPDY	IGLV4-69*01	QTWDTGIVL	p27	—

[a]Western blotting analysis was performed to determine the target viral protein.
[b]Neutralization assay was performed by infection of TZM-bl cells with SIVsmH635FC. Neutralization was shown by % inhibition of infection.
[c](P) pseudogene.
[d]—, < 50% inhibition.

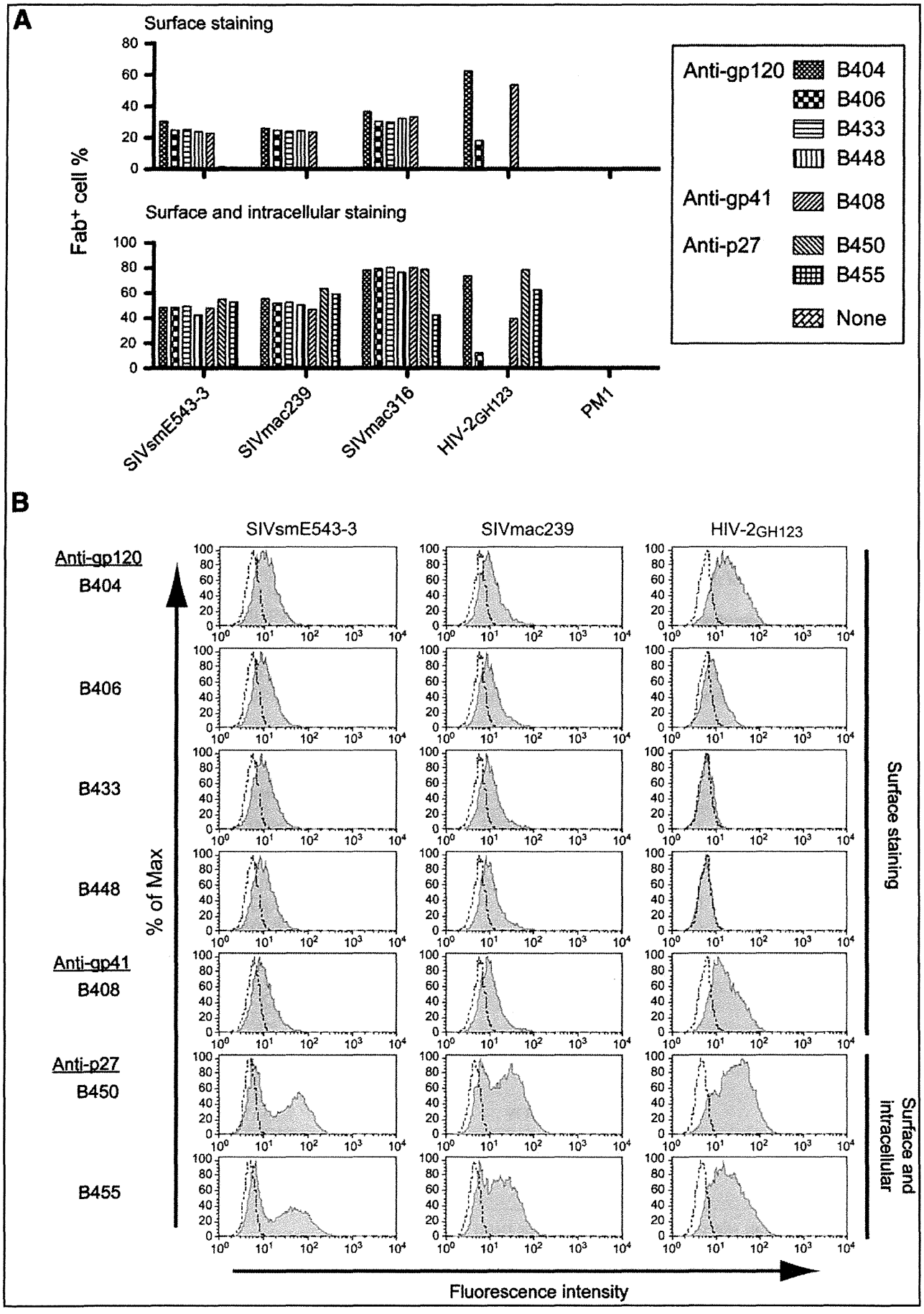
A
Surface staining
Surface and intracellular staining
Fab+ cell %
Anti-gp120
B404
B406
B433
B448
Anti-gp41
B408
Anti-p27
B450
B455
None
SIVsmE543-3
SIVmac239
SIVmac316
HIV-2GH123
PM1
B
SIVsmE543-3
SIVmac239
HIV-2GH123
Anti-gp120
B404
B406
B433
B448
Anti-gp41
B408
Anti-p27
B450
B455
% of Max
Surface staining
Surface and intracellular
Fluorescence intensity

alleles, IGLV3, IGLV4, and IGLV6. Fourteen clones with the IGKV2-40*01 allele showed homologous CDR3 sequences, suggesting that these clones had the same origin.

Western blot assay was performed using crude bacterial supernatants to determine the target protein recognized by the each of these Fab clones (Table 2). Four Fab clones, B404, B406, B433, and B448, recognized Env gp120. Two clones, B450 and B455, recognized Gag p27. The other 14 clones, which had the predominant IGKV sequence, recognized Env gp41. The four anti-gp120 Fab clones were closely related to one another, but two anti-p27 Fab clones had distinct origins (Table 2). Identification of Fab clones against multiple proteins with multiple V gene alleles suggests that the library from SIVsmH635FC-infected macaque, H723, contains a wide variety of Fab genes against SIV.

Reactivity of Fabs to SIV or HIV-2-infected cells

Four anti-gp120 Fabs (B404, B406, B433, and B448), one anti-gp41 Fab (B408), and two anti-p27 Fabs (B450 and B455) were affinity purified and examined for their ability to bind virus-infected cells. Anti-gp120 and anti-gp41 Fabs efficiently bound cells infected with SIVsmE543-3, SIVmac239, and SIVmac316. However, reactivity to HIV-2_{GH123} differed among the Fab clones (Fig. 4A). B404 and B408 showed significant reactivity to HIV-2_{GH123}, whereas very weak to no reactivity was observed for B406, B433, and B448 (Fig. 4A and B). Anti-p27 Fab^+ cells were observed only after permeabilization, consistent with the cytoplasmic localization of the Gag protein (Fig. 4A). These Fabs cross-react with all the SIV strains and HIV-2_{GH123}, though the fluorescence intensity of B455 was low against HIV-2_{GH123} (Fig. 4B). Results showed that these Fabs efficiently bound diverse strains of SIVsm/mac, and some of them were cross-reactive with HIV-2.

Neutralizing activity of anti-gp120 Fabs against various SIV strains

The neutralizing activity of the Fab clones was tested using a neutralization assay against SIVsmH635FC (Table 2). All the crude bacterial supernatants from anti-gp120 Fab clones had high neutralizing activity, though anti-gp41 and anti-Gag Fab clones did not show any inhibitory effect. To analyze the spectrum and potency of neutralizing activity, we examined the capacity of purified Fabs to neutralize other SIV strains, SIVsmE543-3, SIVmac239, and SIVmac316, and HIV-2_{GH123} (Fig. 5). Consistent with the results from crude bacterial supernatants, purified anti-gp120 Fabs, B404, B406, B433, and B448, efficiently neutralized SIVsmH635FC, whereas the anti-gp41 Fab, B408, had no effect. Neutralization of SIVsmH635FC was achieved at a concentration of 16–80 ng/ml for IC_{90} and at 3.2–16 ng/ml for IC_{50} (Fig. 5A).

SIVsmE543-3, which is genetically close to SIVsm H635FC but considerably more resistant to antibody neutralization, was also neutralized by these anti-gp120 Fabs (Fig. 5B). The maximum inhibition of SIVsmE543-3 ranged from 60% to 80%, indicating that its neutralizing activity was moderate compared with that of SIVsmH635FC. However, IC_{50} against SIVsmE543-3 was 3.2 ng/ml, which was the same level as that of SIVsmH635FC. Furthermore, the broad spectrum of these anti-gp120 Fabs was shown by neutralization of the genetically heterologous, neutralization-sensitive SIV strain, SIVmac316 (Fig. 5D). Neutralization of SIVmac316 was similar to that of SIVsmH635FC. The low IC_{50} value against various SIV strains (3.2–16 ng/ml) demonstrated the potency of these Fabs since broad-spectrum anti-HIV-1 NAbs did not neutralize most of the primary HIV-1 strains at less than 10 ng/ml.[7]

SIVmac239, another heterologous strain, and HIV-2_{GH123} were not neutralized by any Fab (Fig. 5C and E). HIV-2_{GH123} was not neutralized, perhaps because of its low cross-reactivity, though B404 bound HIV-2_{GH123} (Fig. 4). Unsuccessful neutralization of SIVmac239 may be related to the Env structure, which is highly resistant to antibody neutralization,[16,17] as well as the antigenic difference between SIVmac239 and SIVsmH635FC.

The neutralization pattern of these anti-gp120 Fabs was similar to that of the plasma sample of the macaque from which the library was constructed (Fig. 5, right panels). The neutralizing activity of H723 plasma was markedly high against SIVsmH635FC and SIVmac316, moderate against SIVsmH543, and extremely low against SIVmac239 and HIV-2_{GH123}. This similarity suggests that anti-gp120 Fabs, B404, B406, B433, and B448, may be representative NAbs in the host macaque.

Anti-gp120 Fab clones share the same epitope on gp120

To identify the epitope recognized by anti-gp120 Fab clones, we performed competition ELISA using IgG-B404, which was converted from Fab B404 to a complete rhesus IgG. The binding and neutralizing ability of IgG-404 was shown to be similar to Fab B404 by ELISA and neutralizing assay (data not shown). In the first experiment, the binding of anti-gp120 Fabs, B404, B406, B433, and B448, was examined in competition with IgG-B404 to determine whether these Fabs recognize the same epitope. As shown in Fig. 6A, all the anti-gp120 Fabs were inhibited with similar kinetics by IgG-B404. This competition suggests that these Fabs recognize the same epitope, or that there is an overlap in their epitopes. In the second experiment, murine MAbs were examined for their binding ability in competition with IgG-B404 to identify the epitope of B404. IgG-B404 competed with three murine MAbs, KK42,

FIG. 4. Ability of Fabs to bind virus-infected cells. Uninfected PM1 cells and PM1 cells that were infected with SIVsmE543-3, SIVmac239, SIVmac316, and HIV-2_{GH123} were incubated with Fab, B404, B406, B433, B448, B408, B450, and B455, and the reactivity of Fab was analyzed by flow cytometry. **(A)** Percentages of cell-surface Fab^+ cells without permeabilization (upper) and Fab^+ cells after staining both surface and intracellular staining by permeabilization (lower) are shown. **(B)** Flow cytometry profiles of PM1 cells infected with SIVsmE543-3, SIVmac239, and HIV-2_{GH123} are shown as representative samples. The results of surface staining were shown in Fab clones against gp120 and gp41, and those of surface and intracellular staining were shown in Anti-p27 Fab, as indicated on the right. The tinted histogram represents cells stained by the Fab indicated on the left. The dotted line shows unstained control.

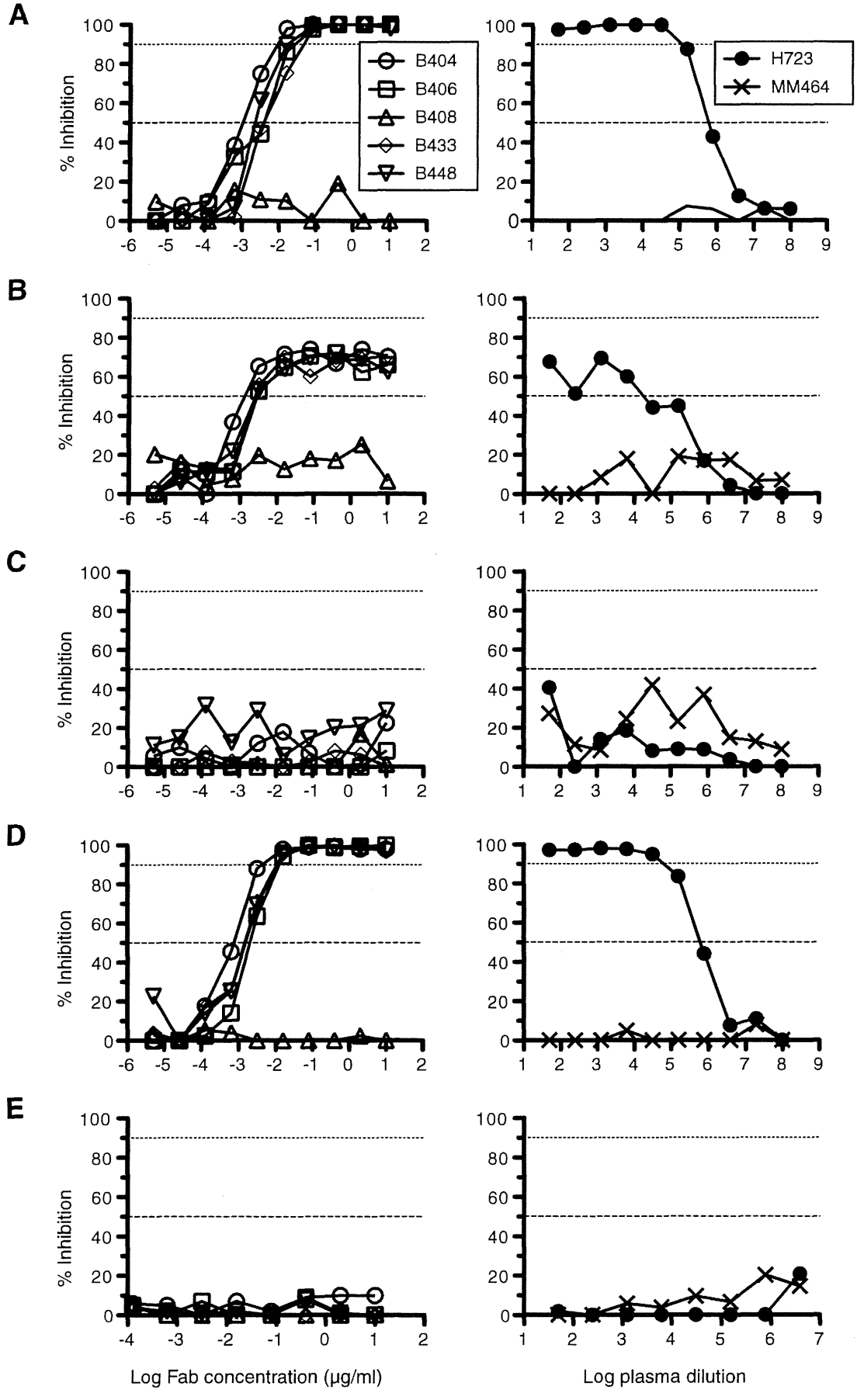
A
B
C
D
E
% Inhibition
B404
B406
B408
B433
B448
H723
MM464
Log Fab concentration (μg/ml)
Log plasma dilution

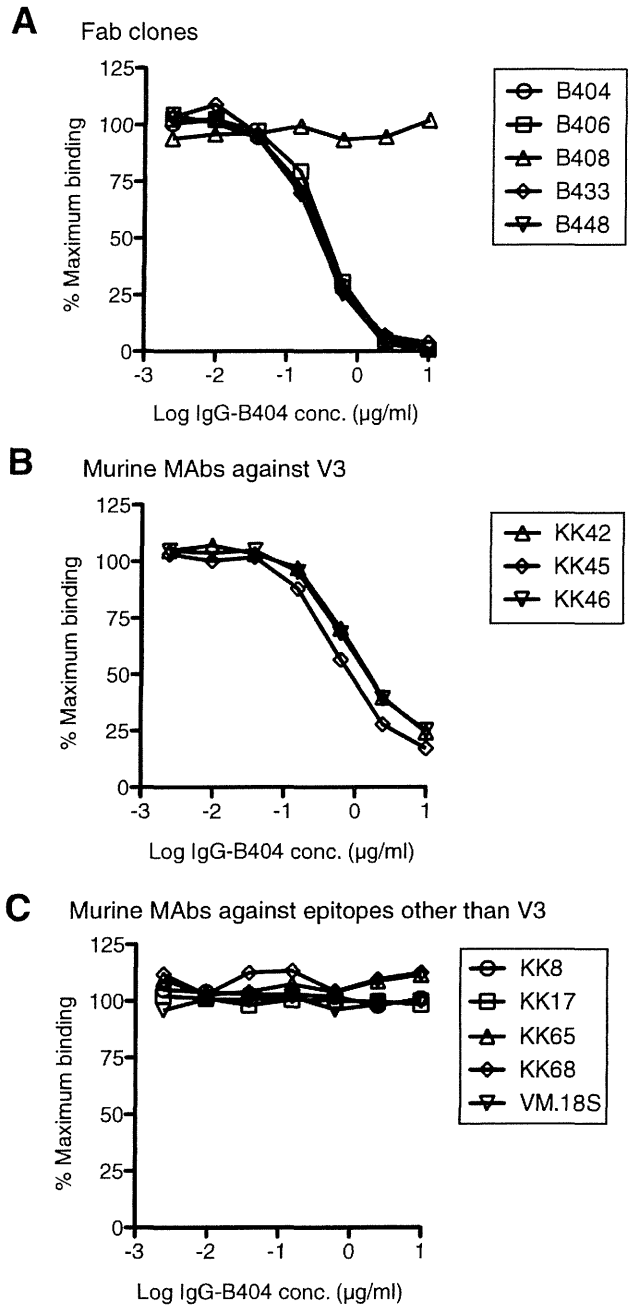

FIG. 6. Identification of epitope specificity of anti-gp120 Fab clones by competition ELISA. **(A)** IgG-B404 inhibited the binding of anti-gp120 Fabs, B404, B406, B433, and B448, but did not inhibit anti-gp41 Fab B406. **(B)** IgG-B404 competed with the binding of murine MAbs, KK42, KK45, and KK46, which recognize a linear epitope in the V3 loop of gp120. **(C)** IgG-B404 did not compete with murine MAbs, KK8 (V1/V2), KK17 (AA8-303), KK65 (V1), KK68 (C1), and VM.18S (unknown).

KK45 and KK46, which all recognize a linear epitope in the V3 loop of gp120 (Fig. 6B). In contrast, IgG-B404 did not compete with murine MAbs that target other epitopes (Fig. 6C). The results suggest that anti-gp120 Fabs, B404, B406, B433, and B448, recognize an epitope containing the V3 loop of gp120.

Discussion

We obtained a panel of MAbs against SIV from an SIV-infected rhesus macaque by using the phage display method. The use of a combinatorial library displayed on the phage surface is an efficient, fast, and well-established strategy to generate MAbs from infected or vaccinated donors.[37] The genomic structure of macaque Ig genes closely resembles that of human and germline sequences of macaque V, D, and J segments and shows high identity with those of humans.[43–51] Therefore, oligonucleotide primers for human Ig variable regions were used to amplify macaque variable regions. In this study, we modified primers for human Ig genes to improve their specificity for rhesus macaques. The successful selection of 20 monoclonal Fabs with multiple targets and origins, one of which is close to the human IGHV pseudogene, suggests that rhesus-specific primers were effective in amplifying sufficiently diverse Ig genes to select antibodies from rhesus macaque. Although identification of unknown germline sequences of rhesus macaque Ig genes is required for further improvement of the amplification system specific to rhesus Ig genes, the primers used in this study would clearly be valuable for constructing libraries to generate new MAbs from rhesus macaques.

Although we generated a diversity of Fab clones to SIV envelope and Gag proteins, Fab clones against gp41 comprised the majority. In addition, anti-gp41 Fab B402 and B405 were repeatedly obtained during the screening. One possible reason for the dominance of anti-gp41 Fab could be a bias in the panning procedure toward Fabs that bound this particular antigen. Apparently, the amount of gp120 was low in the absence of Con A,[38] consistent with the very low signal of anti-gp120 Fabs in ELISA. The signals of two anti-p27 Fabs in ELISA were also low compared with anti-gp41 Fabs, suggesting inefficient binding of p27 on the well. The repeated amplification of phage during panning, which excludes minor populations, might result in the dominance of anti-gp41 Fab, which was advantageous for binding to Ag coated on the plate. Selection of Fabs against particular epitopes may also result from the biased panning. Despite the biased selection, identification of Fabs against Env gp120, gp41, and Gag p27 in this study suggests that panning partially reflects antibody response *in vivo* because these viral proteins are major targets for antibodies in macaque H723 (Fig. 2).

Anti-gp120 Fabs, B404, B406, B433, and B448, showed neutralizing activity against three of the four SIV strains used in this study. Of these SIV strains, SIVsmH543-3 was shown to

FIG. 5. Anti-gp120 Fabs, B404, B406, B433, and B448, neutralized various SIV strains. Neutralizing activity against SIVsmH635 **(A)**, SIVsmE543-3 **(B)**, SIVmac239 **(C)**, SIVmac316 **(D)**, and HIV-2_{GH123} **(E)** was measured using Fabs (left panels) and plasma samples (right panels). Titration curves of percent inhibition of virus infectivity by anti-gp120 Fab clones, B404 (circles), B406 (squares), B433 (diamonds), and B448 (inverted triangles), are shown with anti-gp41 Fab B408 (triangles) as a negative control. A plasma sample from SIVsmH635-infected macaque H723 (black circles), from which the phage library was constructed, is compared with that from normal macaque MM464 (crosses). The 50% and 90% inhibitory doses are shown by the dotted line.

be resistant to antibody neutralization through analysis using sera that broadly neutralize genetically diverse SIV strains.[15] Fab B404, B406, B433, and B448 are the first MAbs that can neutralize SIVsmH543-3. The successful selection of these NAbs against neutralization-resistant SIV may be due to the robust antibody response in H723 from which the Fab library was constructed. H723 was inoculated with SIVsmH635FC, a derivative of SIVsmH543-3. The genomes of SIVsmH543-3 and SIVsmH635FC differ by only 15 nucleotides, but their sensitivities to neutralization are significantly different.[31,32] Inoculation of macaques with neutralization-sensitive SIVsmH635FC resulted in the emergence of revertants to SIVsmH543-3 and variants with diverse V1/V2 and V4 regions.[31] Antibody response to these mutant viruses is consistent with the identification of NAbs against SIVsmH543-3 in H723, though we did not analyze the neutralizing activity of plasma samples from H723 against these mutant viruses.

The relationship between SIVmac239 and SIVmac316 is similar to the relationship between SIVsmH543-3 and SIVsmH635FC in terms of genetic homology and sensitivity to neutralization. SIVmac239 is highly resistant to neutralization by polyclonal antisera or MAbs, though SIVmac316, which is genetically close to SIVmac239, is highly sensitive to neutralization.[16,17] Anti-gp120 Fabs, B404, B406, B433, and B448, showed efficient neutralization against SIVmac316, but no neutralization was observed against SIVmac239. Neutralization of SIVmac316 suggests that B404, B406, B433, and B448 have a broad neutralizing activity against diverse SIV strains because the similarity of the Env amino acid sequence is only 83.1% between SIVsmH635 and SIVmac316. Recognition of a conformational epitope by these anti-gp120 Fabs may make it possible to neutralize various SIV strains. Although the anti-gp120 Fabs were shown to recognize an epitipe including the V3 loop, amino acid sequences in the V3 loop was significantly different among SIV strains and HIV-2, to which these Fabs bound. The panning using antigen by Triton X-100 treatment, which did not cause the destruction of the protein secondary structure, may prompt an efficient selection of Fabs against conformational epitopes. Unsuccessful neutralization of SIVmac239 by these Fabs, despite their ability to bind SIVmac239, simply confirms that this virus is resistant to antibody neutralization. The mechanism of resistance may be similar to that observed in primary HIV-1 strains[8,9,13] and the Env structure would be important for resistance.[16,17]

The present study demonstrates that the phage display method is a powerful tool to obtain MAbs from rhesus macaques. This approach will help to identify antigens and epitopes recognized by the immune response during SIV infection. The use of the SIV virion as an antigen and monoclonal antibodies to capture viral protein will improve the efficiency of obtaining potent neutralizing antibodies. Fab clones with neutralizing activity will be useful to analyze the mechanism of broad neutralization using the SIV macaque model.

Acknowledgments

We thank Dr. Masafumi Takiguchi and his laboratory members for helpful discussion and support for the experiments. We thank Dr. Shinya Suzu for helpful advice about the expression system. The phagemid vector pComb3X was kindly provided by the Scripps Research Institute. The following reagents were obtained through the NIH AIDS Research and Reference Reagent Program, Division of AIDS, NIAID, NIH: PM1 from Dr. Marvin Reitz, GHOST(3) Hi-5 from Dr. Vineet N. KewalRamani and Dr. Dan R. Littman, and TZM-bl from Dr. John C. Kappes, Dr. Xiaoyun Wu, and Tranzyme Inc., KK8, KK17, KK42, KK45, KK46, KK65, and KK68 from Dr. Karen Kent and Miss Caroline Powell, and VM.18S from NIAID, DAIDS. We also thank Dr. Vanessa M. Hirsch for valuable advice. This work was supported in part by the Special Coordination Funds for Promoting Science and Technology from the Ministry of Education, Culture, Sport, Science, and Technology, Japan.

Author Disclosure Statement

No competing financial interests exist.

References

1. Igarashi T, Brown C, Azadegan A, *et al.*: Human immunodeficiency virus type 1 neutralizing antibodies accelerate clearance of cell-free virions from blood plasma. Nat Med 1999;5(2):211–216.
2. Shibata R, Igarashi T, Haigwood N, *et al.*: Neutralizing antibody directed against the HIV-1 envelope glycoprotein can completely block HIV-1/SIV chimeric virus infections of macaque monkeys. Nat Med 1999;5(2):204–210.
3. Veazey RS, Shattock RJ, Pope M, *et al.*: Prevention of virus transmission to macaque monkeys by a vaginally applied monoclonal antibody to HIV-1 gp120. Nat Med 2003;9(3): 343–346.
4. Hessell AJ, Rakasz EG, Poignard P, *et al.*: Broadly neutralizing human anti-HIV antibody 2G12 is effective in protection against mucosal SHIV challenge even at low serum neutralizing titers. PLoS Pathog 2009;5(5):e1000433.
5. Mascola JR, Stiegler G, VanCott TC, *et al.*: Protection of macaques against vaginal transmission of a pathogenic HIV-1/SIV chimeric virus by passive infusion of neutralizing antibodies. Nat Med 2000;6(2):207–210.
6. D'Souza MP, Livnat D, Bradac JA, and Bridges SH: Evaluation of monoclonal antibodies to human immunodeficiency virus type 1 primary isolates by neutralization assays: Performance criteria for selecting candidate antibodies for clinical trials. AIDS Clinical Trials Group Antibody Selection Working Group. J Infect Dis 1997;175(5):1056–1062.
7. Walker LM, Phogat SK, Chan-Hui PY, *et al.*: Broad and potent neutralizing antibodies from an African donor reveal a new HIV-1 vaccine target. Science 2009;326(5950):285–289.
8. Saphire EO, Parren PW, Pantophlet R, *et al.*: Crystal structure of a neutralizing human IGG against HIV-1: A template for vaccine design. Science 2001;293(5532):1155–1159.
9. Karlsson Hedestam GB, Fouchier RA, Phogat S, Burton DR, Sodroski J, and Wyatt RT: The challenges of eliciting neutralizing antibodies to HIV-1 and to influenza virus. Nat Rev Microbiol 2008;6(2):143–155.
10. Li Y, Migueles SA, Welcher B, *et al.*: Broad HIV-1 neutralization mediated by CD4-binding site antibodies. Nat Med 2007;13(9):1032–1034.
11. Haynes BF, Fleming J, St Clair EW, *et al.*: Cardiolipin polyspecific autoreactivity in two broadly neutralizing HIV-1 antibodies. Science 2005;308(5730):1906–1908.
12. Ofek G, McKee K, Yang Y, *et al.*: Relationship between antibody 2F5 neutralization of HIV-1 and hydrophobicity of its heavy chain third complementarity-determining region. J Virol 2010;84(6):2955–2962.

13. Poignard P, Saphire EO, Parren PW, and Burton DR: gp120: Biologic aspects of structural features. Annu Rev Immunol 2001;19:253–274.
14. Hirsch VM and Lifson JD: Simian immunodeficiency virus infection of monkeys as a model system for the study of AIDS pathogenesis, treatment, and prevention. Adv Pharmacol 2000;49:437–477.
15. Hirsch V, Adger-Johnson D, Campbell B, *et al.*: A molecularly cloned, pathogenic, neutralization-resistant simian immunodeficiency virus, SIVsmE543-3. J Virol 1997;71(2):1608–1620.
16. Johnson WE, Sanford H, Schwall L, *et al.*: Assorted mutations in the envelope gene of simian immunodeficiency virus lead to loss of neutralization resistance against antibodies representing a broad spectrum of specificities. J Virol 2003; 77(18):9993–10003.
17. Means RE, Matthews T, Hoxie JA, Malim MH, Kodama T, and Desrosiers RC: Ability of the V3 loop of simian immunodeficiency virus to serve as a target for antibody-mediated neutralization: Correlation of neutralization sensitivity, growth in macrophages, and decreased dependence on CD4. J Virol 2001;75(8):3903–3915.
18. Samuelsson A, Chiodi F, Ohman P, Putkonen P, Norrby E, and Persson MA: Chimeric macaque/human Fab molecules neutralize simian immunodeficiency virus. Virology 1995; 207(2):495–502.
19. Chassagne S, Laffly E, Drouet E, Herodin F, Lefranc MP, and Thullier P: A high-affinity macaque antibody Fab with human-like framework regions obtained from a small phage display immune library. Mol Immunol 2004;41(5):539–546.
20. Glamann J, Burton DR, Parren PW, *et al.*: Simian immunodeficiency virus (SIV) envelope-specific Fabs with high-level homologous neutralizing activity: Recovery from a long-term-nonprogressor SIV-infected macaque. J Virol 1998; 72(1):585–592.
21. Druar C, Saini SS, Cossitt MA, *et al.*: Analysis of the expressed heavy chain variable-region genes of Macaca fascicularis and isolation of monoclonal antibodies specific for the Ebola virus' soluble glycoprotein. Immunogenetics 2005;57(10):730–738.
22. Cole KS, Alvarez M, Elliott DH, *et al.*: Characterization of neutralization epitopes of simian immunodeficiency virus (SIV) recognized by rhesus monoclonal antibodies derived from monkeys infected with an attenuated SIV strain. Virology 10 2001;290(1):59–73.
23. Robinson JE, Cole KS, Elliott DH, *et al.*: Production and characterization of SIV envelope-specific rhesus monoclonal antibodies from a macaque asymptomatically infected with a live SIV vaccine. AIDS Res Hum Retroviruses 1998;14(14): 1253–1262.
24. Lusso P, Cocchi F, Balotta C, *et al.*: Growth of macrophage-tropic and primary human immunodeficiency virus type 1 (HIV-1) isolates in a unique CD4+ T-cell clone (PM1): Failure to downregulate CD4 and to interfere with cell-line-tropic HIV-1. J Virol 1995;69(6):3712–3720.
25. Takeuchi Y, McClure MO, and Pizzato M: Identification of gammaretroviruses constitutively released from cell lines used for human immunodeficiency virus research. J Virol 2008;82(24):12585–12588.
26. Wei X, Decker JM, Liu H, *et al.*: Emergence of resistant human immunodeficiency virus type 1 in patients receiving fusion inhibitor (T-20) monotherapy. Antimicrob Agents Chemother 2002;46(6):1896–1905.
27. Derdeyn CA, Decker JM, Sfakianos JN, *et al.*: Sensitivity of human immunodeficiency virus type 1 to the fusion inhibitor T-20 is modulated by coreceptor specificity defined by the V3 loop of gp120. J Virol 2000;74(18):8358–8367.
28. Platt EJ, Wehrly K, Kuhmann SE, Chesebro B, and Kabat D: Effects of CCR5 and CD4 cell surface concentrations on infections by macrophagetropic isolates of human immunodeficiency virus type 1. J Virol 1998;72(4):2855–2864.
29. Morner A, Bjorndal A, Albert J, *et al.*: Primary human immunodeficiency virus type 2 (HIV-2) isolates, like HIV-1 isolates, frequently use CCR5 but show promiscuity in coreceptor usage. J Virol 1999;73(3):2343–2349.
30. DuBridge RB, Tang P, Hsia HC, Leong PM, Miller JH, and Calos MP: Analysis of mutation in human cells by using an Epstein-Barr virus shuttle system. Mol Cell Biol 1987;7(1): 379–387.
31. Kuwata T, Byrum R, Whitted S, *et al.*: A rapid progressor-specific variant clone of simian immunodeficiency virus replicates efficiently in vivo only in the absence of immune responses. J Virol 2007;81(17):8891–8904.
32. Kuwata T, Dehghani H, Brown CR, *et al.*: Infectious molecular clones from a simian immunodeficiency virus-infected rapid-progressor (RP) macaque: Evidence of differential selection of RP-specific envelope mutations in vitro and in vivo. J Virol 2006;80(3):1463–1475.
33. Kuwata T, Nishimura Y, Whitted S, *et al.*: Association of progressive CD4(+) T cell decline in SIV infection with the induction of autoreactive antibodies. PLoS Pathog 2009;5(4): e1000372.
34. Kestler H, Kodama T, Ringler D, *et al.*: Induction of AIDS in rhesus monkeys by molecularly cloned simian immunodeficiency virus. Science 1990;248(4959):1109–1112.
35. Mori K, Ringler DJ, Kodama T, and Desrosiers RC: Complex determinants of macrophage tropism in env of simian immunodeficiency virus. J Virol 1992;66(4):2067–2075.
36. Shibata R, Miura T, Hayami M, *et al.*: Mutational analysis of the human immunodeficiency virus type 2 (HIV-2) genome in relation to HIV-1 and simian immunodeficiency virus SIV (AGM). J Virol 1990;64(2):742–747.
37. Barbas CF, Scott JM, Silverman G, and Burton DR: *Phage Display: A Laboratory Manual.* Cold Spring Harbor Laboratory Press, Cold Spring Harbor, NY, 2001.
38. Robinson JE, Holton D, Liu J, McMurdo H, Murciano A, and Gohd R: A novel enzyme-linked immunosorbent assay (ELISA) for the detection of antibodies to HIV-1 envelope glycoproteins based on immobilization of viral glycoproteins in microtiter wells coated with concanavalin A. J Immunol Methods 1990;132(1):63–71.
39. Kent KA, Gritz L, Stallard G, *et al.*: Production and of monoclonal antibodies to simian immunodeficiency virus envelope glycoproteins. AIDS 1991;5(7):829–836.
40. Kent KA, Rud E, Corcoran T, *et al.*: Identification of two neutralizing and 8 non-neutralizing epitopes on simian immunodeficiency virus envelope using monoclonal antibodies. AIDS Res Hum Retroviruses 1992;8(6):1147–1151.
41. Lefranc MP, Giudicelli V, Ginestoux C, *et al.*: IMGT, the international ImMunoGeneTics information system. Nucleic Acids Res 2009;37(Database issue):D1006–1012.
42. Ourmanov I, Kuwata T, Goeken R, *et al.*: Improved survival in rhesus macaques immunized with modified vaccinia virus Ankara recombinants expressing simian immunodeficiency virus envelope correlates with reduction in memory CD4+ T-cell loss and higher titers of neutralizing antibody. J Virol 2009;83(11):5388–5400.
43. Andris JS, Miller AB, Abraham SR, *et al.*: Variable region gene segment utilization in rhesus monkey hybridomas

producing human red blood cell-specific antibodies: Predominance of the VH4 family but not VH4-21 (V4-34). Mol Immunol 1997;34(3):237–253.
44. Bible JM, Howard W, Robbins H, and Dunn-Walters DK: IGHV1, IGHV5 and IGHV7 subgroup genes in the rhesus macaque. Immunogenetics 2003;54(12):867–873.
45. Ermert K, Mitlohner H, Schempp W, and Zachau HG: The immunoglobulin kappa locus of primates. Genomics 1995; 25(3):623–629.
46. Helmuth EF, Letvin NL, and Margolin DH: Germline repertoire of the immunoglobulin V(H)3 family in rhesus monkeys. Immunogenetics 2000;51(7):519–527.
47. Howard WA, Bible JM, Finlay-Dijsselbloem E, Openshaw S, and Dunn-Walters DK: Immunoglobulin light-chain genes in the rhesus macaque I: Kappa light-chain germline sequences for subgroups IGKV1, IGKV and IGKV3. Immunogenetics 2005;57(3–4):210–218.
48. Howard WA, Bible JM, Finlay-Dijsselbloem E, Openshaw S, and Dunn-Walters DK: Immunoglobulin light-chain genes in the rhesus macaque II: Lambda light-chain germline sequences for subgroups IGLV1, IGLV2, IGLV3, IGLV4 and IGLV5. Immunogenetics 2005;57(9): 655–664.
49. Link JM, Hellinger MA, and Schroeder HW Jr: The rhesus monkey immunoglobulin IGHD and IGHJ germline repertoire. Immunogenetics 2002;54(4):240–250.
50. Link JM, Larson JE, and Schroeder HW: Despite extensive similarity in germline DH and JH sequence, the adult rhesus macaque CDR-H3 repertoire differs from human. Mol Immunol 2005;42(8):943–955.
51. Scinicariello F, Engleman CN, Jayashankar L, McClure HM, and Attanasio R: Rhesus macaque antibody molecules: Sequences and heterogeneity of alpha and gamma constant regions. Immunology 2004;111(1):66–74.
52. Gibbs RA, Rogers J, Katze MG, *et al.*: Evolutionary and biomedical insights from the rhesus macaque genome. Science 2007;316(5822):222–234.

Address correspondence to:
Takeo Kuwata
Priority Organization for Innovation and Excellence
Kumamoto University
Honjyo-Kyoyo-to Rm208
2-2-1 Honjyo
Kumamoto 860-0811
Japan
E-mail: tkuwata@kumamoto-u.ac.jp

JOURNAL OF VIROLOGY, Oct. 2011, p. 10617–10626 Vol. 85, No. 20
0022-538X/11/$12.00 doi:10.1128/JVI.05010-11

Recombination-Mediated Changes in Coreceptor Usage Confer an Augmented Pathogenic Phenotype in a Nonhuman Primate Model of HIV-1-Induced AIDS▽†

Yoshiaki Nishimura,[1] Masashi Shingai,[1] Wendy R. Lee,[1] Reza Sadjadpour,[1] Olivia K. Donau,[1] Ronald Willey,[1] Jason M. Brenchley,[1] Ranjini Iyengar,[1] Alicia Buckler-White,[1] Tatsuhiko Igarashi,[2] and Malcolm A. Martin[1]*

Laboratory of Molecular Microbiology, National Institute of Allergy and Infectious Diseases, National Institutes of Health, Bethesda, Maryland 20892,[1] and Laboratory of Primate Models, Institute for Virus Research, Kyoto University, 53 Shogoinkawaramachi, Sakyo-ku, Kyoto 606-8507, Japan[2]

Received 2 May 2011/Accepted 27 July 2011

Evolution of the *env* gene in transmitted R5-tropic human immunodeficiency virus type 1 (HIV-1) strains is the most widely accepted mechanism driving coreceptor switching. In some infected individuals, however, a shift in coreceptor utilization can occur as a result of the reemergence of a cotransmitted, but rapidly controlled, X4 virus. The latter possibility was studied by dually infecting rhesus macaques with X4 and R5 chimeric simian simian/human immunodeficiency viruses (SHIVs) and monitoring the replication status of each virus using specific primer pairs. In one of the infected monkeys, both SHIVs were potently suppressed by week 12 postinoculation, but a burst of viremia at week 51 was accompanied by an unrelenting loss of total CD4$^+$ T cells and the development of clinical disease. PCR analyses of plasma viral RNA indicated an *env* gene segment containing the V3 region from the inoculated X4 SHIV had been transferred into the genetic background of the input R5 SHIV by intergenomic recombination, creating an X4 virus with novel replicative, serological, and pathogenic properties. These results indicate that the effects of retrovirus recombination *in vivo* can be functionally profound and may even occur when one of the recombination participants is undetectable in the circulation as cell-free virus.

Human immunodeficiency virus type 1 (HIV-1) infections of humans and simian immunodeficiency virus (SIV) infections of macaques are both initiated by the binding of virions to CD4 receptors present on the surface of target cells. In addition to CD4, both primate lentiviruses require a second receptor (or coreceptor) for successful cell entry (1). For HIV-1, the chemokine receptors CCR5 and CXCR4 are the major coreceptors. *In vivo*, the predominant HIV-1 population detected in the blood in recently infected individuals utilizes the CCR5 receptor (and are designated R5 viruses) (51, 55, 60). In a large fraction of individuals infected with HIV-1 subtypes B and D, virus strains capable of using CXCR4 (X4 viruses) or both CCR5 and CXCR4 (R5/X4 viruses) have been recovered from the plasma during the late phase of the chronic infection (6, 22). This shift has been termed "coreceptor switching" and is frequently associated with a more rapid loss of CD4$^+$ T cells and an accelerated clinical course (6, 44).

Several mechanisms have been proposed to explain the change in HIV-1 coreceptor utilization (40). Genetic evolution of the *env* gene present in the transmitted R5 virus, facilitated by the error-prone nature of the HIV-1 reverse transcriptase, is the most widely accepted explanation for coreceptor switching. This mechanism is consistent with the predominance of R5 HIV-1 strains during the asymptomatic phase of the infection, as well as the resistance of individuals, homozygous for a 32-bp deletion of the CCR5 allele (*ccr5-Δ32*), to HIV infection (7, 50). Point mutations affecting the gp120 V3 loop that introduce positively charged amino acids at positions 11, 24, and 25 have been associated with the shifted utilization of the CXCR4 chemokine receptor, although changes in other regions of the *env* gene may also contribute to this process (8, 11, 14, 21, 39, 43). A second mechanism to explain coreceptor switching proposes that X4 and R5 HIV-1 strains are both transmitted to new recipients, but the X4 viruses are more readily controlled and are not detected in the plasma during the asymptomatic phase of the infection, remaining suppressed as long as the immune system is functional (40, 53). As immune competence wanes, the previously constrained X4 and/or dualtropic viruses replicate more freely and begin targeting naive CD4$^+$ T lymphocytes for depletion.

Although pathogenic SIVs have been reported to use a plethora of non-CXCR4 coreceptors in addition to CCR5 (27), they are predominantly R5-tropic in macaque cells, and coreceptor switching has rarely been reported (25, 33, 59). In contrast, there have been several reports of coreceptor switching in rhesus monkeys infected with R5-tropic SHIVs (12, 13, 34, 42). However, in contrast to the delayed emergence of X4- or R5/X4-tropic viruses in HIV-1-infected individuals, all of the R5-SHIV-infected animals have been rapid progressors and the coreceptor switch occurred within a few months of virus inoculation (2).

* Corresponding author. Mailing address: Bldg. 4, Rm. 315A, 4 Center Dr., MSC 0460, National Institutes of Health, Bethesda, MD 20892-0460. Phone: (301) 496-4012. Fax: (301) 402-0226. E-mail: malm@nih.gov.

† Supplemental material for this article may be found at http://jvi.asm.org/.

▽ Published ahead of print on 3 August 2011.

In this report, we have studied the reemergence mechanism of coreceptor switching by dually infecting rhesus monkeys with X4 and R5 SHIVs. Envelope-specific primer pairs and probes were used to individually monitor each virus strain *in vivo*. In one of the inoculated animals, the replication of the input X4 and R5 SHIVs, measured by levels of viral RNA in the plasma, was suppressed to the limits of detection by week 12 postinoculation (p.i.). Nonetheless, this monkey experienced a transient burst of virus production at week 25 and a sustained surge of viremia after week 51 p.i., which was accompanied by a marked decline in the number of circulating $CD4^+$ T lymphocytes and death from immunodeficiency at week 100 p.i. In this normally progressing macaque, a recombination event occurred between weeks 25 and 50, which transferred an *env* gene segment that included the V3 region from the starting X4-tropic SHIV into the genetic background of the input R5 SHIV, and created a novel X4 virus with augmented replicative and pathogenic properties. Single genome amplification (SGA) revealed additional recombination events affecting two regions of gp41 and a 142-nucleotide (nt) segment encompassing *tat*, *rev*, and *vpu* gene sequences. In all cases, the gene sequences were transferred unidirectionally from the X4 SHIV input virus into the R5 SHIV genome. Interestingly, high levels of neutralizing antibodies (NAbs) directed against the starting X4-tropic SHIV contributed to its durable suppression by week 10 p.i. In contrast, no NAbs were detected against the starting R5-tropic SHIV or the novel recombinant X4 SHIV that emerged after week 50 p.i., which accelerated progression to AIDS.

MATERIALS AND METHODS

Virus and animal experiments. The construction and characterization of the $SHIV_{DH12R\text{-}Clone\ 7}$ ($SHIV_{DH12R\text{-}CL\text{-}7}$), $SHIV_{DH12R\text{-}CL\text{-}8}$, and SIV_{mac239} molecular clones and their use to generate virus stocks have been described previously (18, 46, 52). The origin and preparation of the tissue culture-derived $SHIV_{AD8\#2}$ have been previously reported (34). The 50% tissue culture infective doses ($TCID_{50}$) of $SHIV_{DH12R\text{-}CL\text{-}8}$ and $SHIV_{AD8\#2}$ were determined by infecting rhesus macaque peripheral blood mononuclear cells (PBMC) in quadruplicate with serial 4-fold dilutions of the animal challenge stocks and then assaying for the reverse transcription (RT) activities in the culture supernatants on day 14 for RT activity (58). Rhesus macaques (*Macaca mulatta*) were maintained in accordance with the guidelines of the Committee on the Care and Use of Laboratory Animals (30) and were housed in a biosafety level 2 facility; biosafety level 3 practices were followed. Phlebotomies, intravenous virus inoculations, euthanasia, and tissue sample collections were performed as previously described (10).

Quantitation of plasma viral RNA and cell associated viral DNA levels. SIV gag RNA levels in plasma or cell-associated viral DNA frequencies in PBMC were determined by real-time RT-PCR (ABI Prism 7700 sequence detection system; Applied Biosystems, Foster City, CA), respectively, as previously reported (10). SIV-, $SHIV_{DH12}$-, or $SHIV_{AD8}$-derived RNAs were separately monitored in dually infected rhesus monkeys by using primer pairs and probes specific for the *env* gene present in each virus, as shown in Table S1 in the supplemental material.

Lymphocyte immunophenotyping and intracellular cytokine assays. EDTA-treated blood samples were stained for flow cytometric analysis as described previously using combinations of the following fluorochrome-conjugated monoclonal antibodies (MAbs): CD3 (fluorescein isothiocyanate [FITC] or phycoerythrin [PE]), CD4 (PE, peridinin chlorophyll protein-Cy5.5 [PerCP-Cy5.5] or allophycocyanin [APC]), CD8 (PerCP or APC), CD28 (FITC or PE), and CD95 (APC) (31, 32).

For intracellular cytokine assays, immune stimulation using SIVmac239 Gag peptides 15 amino acids in length was performed on frozen lymphocytes as described previously (34, 38).

SGA of plasma virus RNA. SGA and direct sequencing were used to characterize and quantitate circulating virus populations in macaque CE43 at various times p.i., as previously described (48), with the following modifications. Plasma viral RNA was extracted by using a QIAamp viral RNA minikit (Qiagen) and then reverse transcribed using SuperScript III First-Strand Synthesis SuperMix (Invitrogen). cDNA was serially diluted to identify a dilution at which PCR-positive wells constituted <30% of the total number of reactions. After direct sequencing, any sequence with mixed bases was excluded. First-round PCR amplifications were performed using the following PCR parameters: 1 cycle of 94°C for 2 min; 40 cycles of a denaturing step of 94°C for 20 s, an annealing step of 55°C for 30 s, and an extension step of 68°C for 1 or 2 min; followed by a final extension of 68°C for 5 min. Second-round PCR amplifications were performed with 2 μl from the first-round PCR products. The second-round PCR was performed under the conditions used for the first-round PCR. The primer sets used for the V3, gp41, and vpu regions are indicated in Table S1 in the supplemental material. Amplified gene segments were directly sequenced by using an Applied Biosystems 3130XL genetic analyzer.

Construction of replication-competent viruses used in coreceptor utilization assays. Full-length infectious molecular clones, containing the entire *env* genes of SHIVs circulating in macaques DB3T and DB3N at week 2 p.i., were constructed by RT-PCR amplification of plasma viral RNA, as previously described (34). The 3,040-bp amplified products, which included the entire *env* gene, were cloned into the EcoRI and SalI (newly created) sites of pSHIVAD8. The two replication-competent SHIVs clones obtained were designated $SHIV_{AD8\text{-}ES3T7}$ and $SHIV_{AD8\text{-}ES3N6}$.

Coreceptor utilization assays in macaque PBMC. Rhesus monkey PBMC (10^5 cells in 100 μl of RPMI 1640) were dispensed in triplicate in 96-well round-bottom plates as previously described (17). CCR5 (AD101)- or CXCR4 (AMD3100)-specific inhibitors (8 μM) in 25 μl was added to each well, followed by incubation for 1 h at 37°C. Test virus (multiplicity of infection = 0.01) in 75 μl was then spinoculated (36) onto the cells at 1,200 × *g* for 1 h at 37°C, and the cultures were maintained for 14 days. One-half (100 μl) of the culture supernatant was replaced daily with fresh medium containing 1 μM coreceptor inhibitor in 0.2% dimethyl sulfoxide (DMSO). Control cultures without inhibitors were maintained with medium containing 0.2% DMSO. The daily supernatant samples collected were monitored for progeny virus production by ^{32}P RT assay as previously described (58).

Virus replication assay in rhesus monkey PBMC. The preparation and infection of rhesus monkey PBMC have been previously described (34). Briefly, PBMC stimulated with concanavalin A and cultured in the presence of recombinant human interleukin-2 were spinoculated (1,200 × *g* for 1 h) (36) with virus normalized for RT activity. Virus replication was assessed by an RT assay of the culture supernatant as described above.

Virus neutralization assays. Virus neutralization assays were performed as previously described (34). Briefly, plasma samples (1:20 dilution) from the monkey CE43 were incubated with virus in quadruplicate in 96-well flat-bottom culture plates in a total volume of 50 μl for 1 h at 37°C. Prechallenge plasma samples from each animal served as controls. Freshly trypsin-treated TZM-bl cells were added, cultures were maintained for an additional 28 h, and intracellular luciferase activity was measured as previously described (57). Any sample resulting in a 50% reduction of luciferase activity compared to that obtained with the uninfected control sample was considered positive for NAbs.

RESULTS

Emergence of a highly pathogenic virus in a macaque dually inoculated with R5 and X4 SHIVs. Although it is currently accepted that the slow evolution of R5-tropic HIV-1 *env* genes is the major pathway driving coreceptor switching in chronically infected individuals, the reemergence of cotransmitted, but durably suppressed, X4 viral strains has also been proposed as an alternative mechanism (28, 40). To evaluate this second mechanism, monkeys were dually infected with an attenuated derivative of the X4-tropic $SHIV_{DH12}$ ($SHIV_{DH12R\text{-}CL\text{-}8}$ [46]) and the recently described R5-tropic $SHIV_{AD8\#2}$ (34). In some of these inoculated macaques, this virus combination resulted in the rapid and complete loss of both naive and memory $CD4^+$ T cells during the acute infection, a finding reminiscent of the "CD4 crash" observed with the highly pathogenic X4 $SHIV_{89.6P}$ and $SHIV_{DH12R}$ (19, 41). To circumvent this problem, a low dose (75 $TCID_{50}$) of $SHIV_{DH12R\text{-}CL\text{-}8}$ was coinoculated with the R5-tropic $SHIV_{AD8\#2}$ (7,500 $TCID_{50}$) to mini-

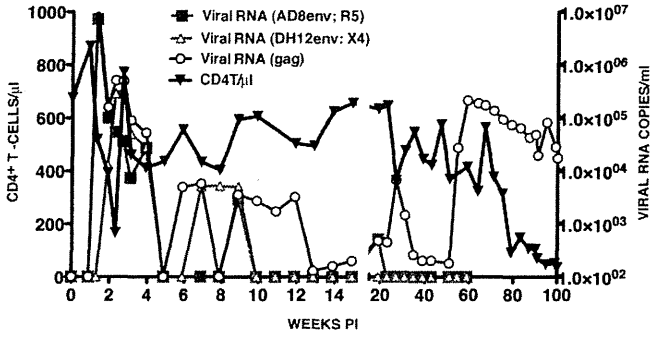

FIG. 1. Plasma viremia and CD4$^+$ T cell levels in a rhesus monkey dually infected with X4- and R5-tropic SHIVs. Macaque CE43 was inoculated intravenously with the X4-tropic $SHIV_{DH12}$ and the R5-tropic $SHIV_{AD8}$. Plasma viral RNA levels were measured using *env* gene primer pairs specific for each SHIV or *gag* gene primer pairs able to detect both viruses. The numbers of total circulating CD4$^+$ T cells were determined during the 100 weeks of infection by flow cytometry.

mize the massive loss of naive and memory CD4$^+$ T cells. Three different primer pair sets were used to measure plasma viral RNA in these infected monkeys: (i) an HIV-1 gp41 membrane-spanning pair, specific for the R5 SHIV; (ii) an HIV-1 gp120 V5 pair, specific for the X4-tropic SHIV; and (iii) an SIV *gag* gene pair for detecting both SHIVs.

One of the dually infected animals (CE43), which did not experience the complete loss of CD4$^+$ T cells acutely, generated peak levels of R5 SHIV viremia on day 10 p.i. and peak X4 SHIV viral RNA loads on 14 p.i. (Fig. 1). A composite viral RNA profile was observed using the SIV *gag* gene primers. Both SHIVs were rapidly and effectively controlled by week 10 p.i., as monitored with the *env* gene primer pairs, and at week 15 the total viral RNA in the plasma was barely (200 RNA copies/ml) above the limits of detection (100 RNA copies/ml) using the *gag* primer pairs. At the conclusion of this early phase of the infection, the numbers of circulating CD4$^+$ T cells were similar to those measured at the time of virus inoculation (Fig. 1).

After week 15, virus replication gradually increased and peaked (10^4 RNA copies/ml) at week 27 p.i., using the *gag* gene primers to monitor plasma viral RNA loads. This increase in plasma viremia was not detectable with *env* gene primer pairs specific for either the X4-tropic or the R5-tropic SHIVs. A second much larger and sustained burst of virus replication, also only detectable with the *gag* primers, occurred after week 51 and peaked (2.2×10^5 RNA copies/ml) at week 59 p.i. The resulting elevated levels of plasma viremia were accompanied by a marked decline of naive CD4$^+$ T lymphocytes (from 168 cells/µl at week 59 to 23 cells/µl at week 71 and 8 cells/µl at week 75). This precipitous loss of naive CD4$^+$ T cells was followed by a downhill clinical course characterized by protracted anorexia, severe diarrhea, and marked weight loss, beginning at week 90 p.i., and required euthanasia of monkey CE43 at week 100. Necropsy revealed the existence of *Pneumocystis carinii* pneumonia; in addition, *Entamoeba* species were visualized on direct fecal smear samples.

The sudden and sustained increase in plasma viremia after week 51 p.i., coupled with the irreversible loss of naive CD4$^+$ T lymphocytes and the onset of clinical disease, suggested that a highly pathogenic virus population had emerged in macaque CE43. Accordingly, 10 ml of blood collected at the time of euthanasia was inoculated intravenously into two recipient animals (DB3T and DB3N). High levels of peak viremia were measurable in both of these monkeys between weeks 2 and 3 p.i. (Fig. 2). An extremely rapid and complete loss of naive and memory CD4$^+$ T lymphocytes occurred in macaque DB3T, requiring euthanasia at week 22 because of intractable diarrhea and marked weight loss. Animal DB3N also experienced a massive depletion of its naive CD4$^+$ T cells (from 1,200 cells/µl at week 0 to 40 cells/µl at week 7) and yet was able to control its set-point viremia to more modest levels and to preserve its memory CD4$^+$ T cells. The rapid elimination of naive CD4$^+$ T lymphocytes in these two recipients of blood from macaque CE43 is similar to the results described previously for animals dually inoculated with high doses of X4-tropic SHIVs.

A coreceptor switch mediated by intergenomic X4 and R5 SHIV recombination occurred in macaque CE43. The extraordinarily rapid depletion of naive CD4$^+$ T lymphocytes in the dually infected macaque CE43 and in two of its immediate blood transfusion recipients suggested that a highly virulent X4 SHIV had emerged in animal CE43 even though the X4

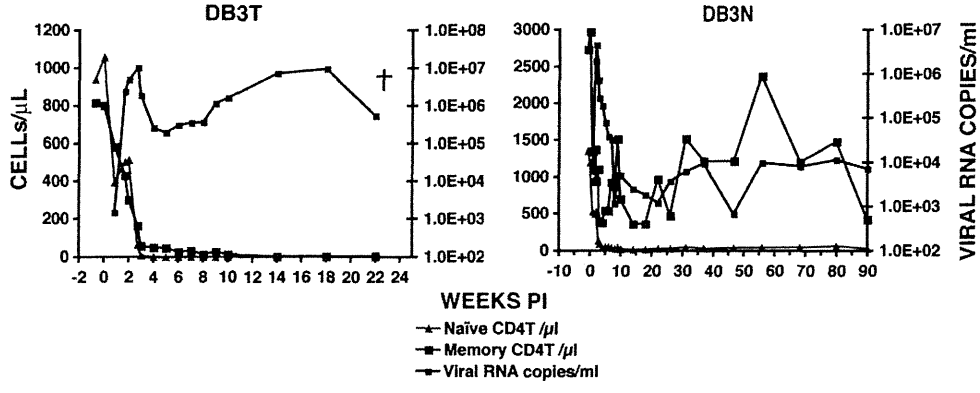

FIG. 2. The transfer of blood from macaque CE43 causes the rapid loss of naive CD4$^+$ T cells in two recipient animals. Portions (10 ml) of blood, collected from macaque CE43 at the time of euthanasia, were transfused into macaques DB3T and DB3N, and the levels of plasma viremia and CD4$^+$ T cell subsets were determined.

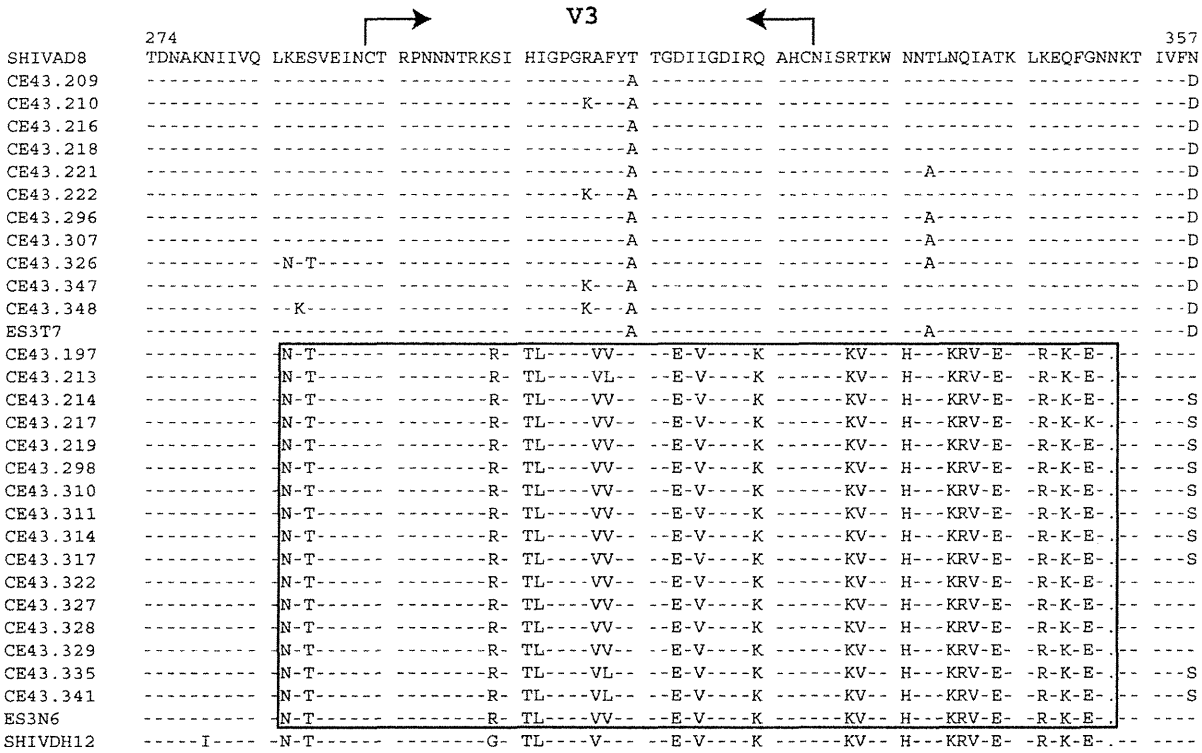

FIG. 3. Two populations of circulating SHIVs bearing distinctive V3 regions are present in the dually infected macaque CE43 at the time of its euthanasia. SGA and direct sequencing of plasma samples collected at week 100 p.i. were used to generate amplicons containing the gp120 V3 region. The bracketed sequences include the V3 region derived from the starting X4-tropic $SHIV_{DH12}$. The gp120 amino acid sequences present in the inoculated $SHIV_{AD8}$ and $SHIV_{DH12}$ are shown in the top and bottom lines, respectively. The ES3T7 and ES3N6 sequences were amplified from the plasma of macaques DB3T and DB3N (see Fig. 2), respectively, at week 2 p.i. The opposing arrows indicate the location of the V3 loop.

$SHIV_{DH12R\text{-}CL\text{-}8}$ it was inoculated with was undetectable after week 10 p.i. (see Fig. 1). SGA was therefore used to characterize the virus present in plasma at the time of euthanasia (week 100 p.i.). As shown in Fig. 3, this analysis revealed the existence of two SHIV populations bearing distinctive *env* genes. One population, the product of X4 SHIV/R5 SHIV intergenomic recombination, carried a 220+-nt segment, which included the entire 105-nt V3 region from the starting X4 $SHIV_{DH12}$ that had been inserted into $SHIV_{AD8}$ *env* gene. The second population carried a V3 region similar to that present in the original R5-tropic $SHIV_{AD8}$. At week 100 when macaque CE43 was euthanized, 59% (16 of 27 amplicons) carried a V3 region resembling that of the inoculated X4-tropic $SHIV_{DH12}$ and 41% (11 of 27 amplicons) bore a V3 gene segment similar to that present in the original R5-tropic SHIV. In addition, two gene segments from the gp41 coding region of the starting X4-tropic SHIV (Fig. 4, underlined DH12 [X4]-A and DH12 [X4]-B amino acid sequences) had been inserted into analogous positions of the $SHIV_{AD8}$ *env* genes of both virus populations.

Coreceptor usage properties of the recombinant SHIVs that emerged in macaque CE43. Not unexpectedly, RT-PCR, cloning, and sequence analyses of plasma collected at week 2 p.i. from the recipients (monkeys DB3N and DB3T) of the CE43 blood transfusion revealed the presence of nearly equal numbers of the two circulating recombinant SHIV populations (data not shown). Full-length replication competent SHIV molecular clones were constructed, which contained an entire *env* gene, amplified from the week 2 plasma samples collected from macaque DB3T or macaque DB3N (designated ES3T7 and ES3N6, respectively, in the gp120 V3 alignments presented in Fig. 3). The coreceptor utilization properties of the resulting SHIVs ($SHIV_{AD8\text{-}ES3T7}$ and $SHIV_{AD8\text{-}ES3N6}$) were assayed in a 14-day replication assay in the presence of CCR5 or CXCR4 small molecule inhibitors. As shown in Fig. 5, replication of the R5-tropic SIVmac239 and the X4-tropic $SHIV_{DH12R\text{-}CL\text{-}7}$ controls was completely blocked by the CCR5- and CXCR4-specific inhibitors, respectively, as previously reported (17). In this assay, the R5 inhibitor suppressed replication of $SHIV_{AD8\text{-}ES3T7}$, which carries a gp120 V3 region similar to that present in the R5-tropic SHIVAD8 inoculum. In contrast, the replication of $SHIV_{AD8\text{-}ES3N6}$, which contains a gp120 V3 region similar to the input X4-tropic $SHIV_{DH12R\text{-}CL\text{-}8}$, was blocked by the X4 inhibitor. Taken together, these results show that the recombination-mediated insertion of an X4 gp120 determinant into the genetic background to a CCR5-utilizing *env* gene was sufficient to shift coreceptor utilization.

Timing of the X4/R5 SHIV intergenomic recombinations during *in vivo* infection. SGA and direct sequencing were used to characterize and quantitate circulating virus populations at various times following the dual inoculation of macaque CE43 with X4-tropic and R5-tropic SHIVs. The results obtained are summarized in Fig. 6. At week 31 p.i., a single circulating SHIV species was identified in the burst of virus replication that was undetectable by RT-PCR of the plasma samples, using either of the two *env*-specific primer pairs (see Fig. 1). All of the

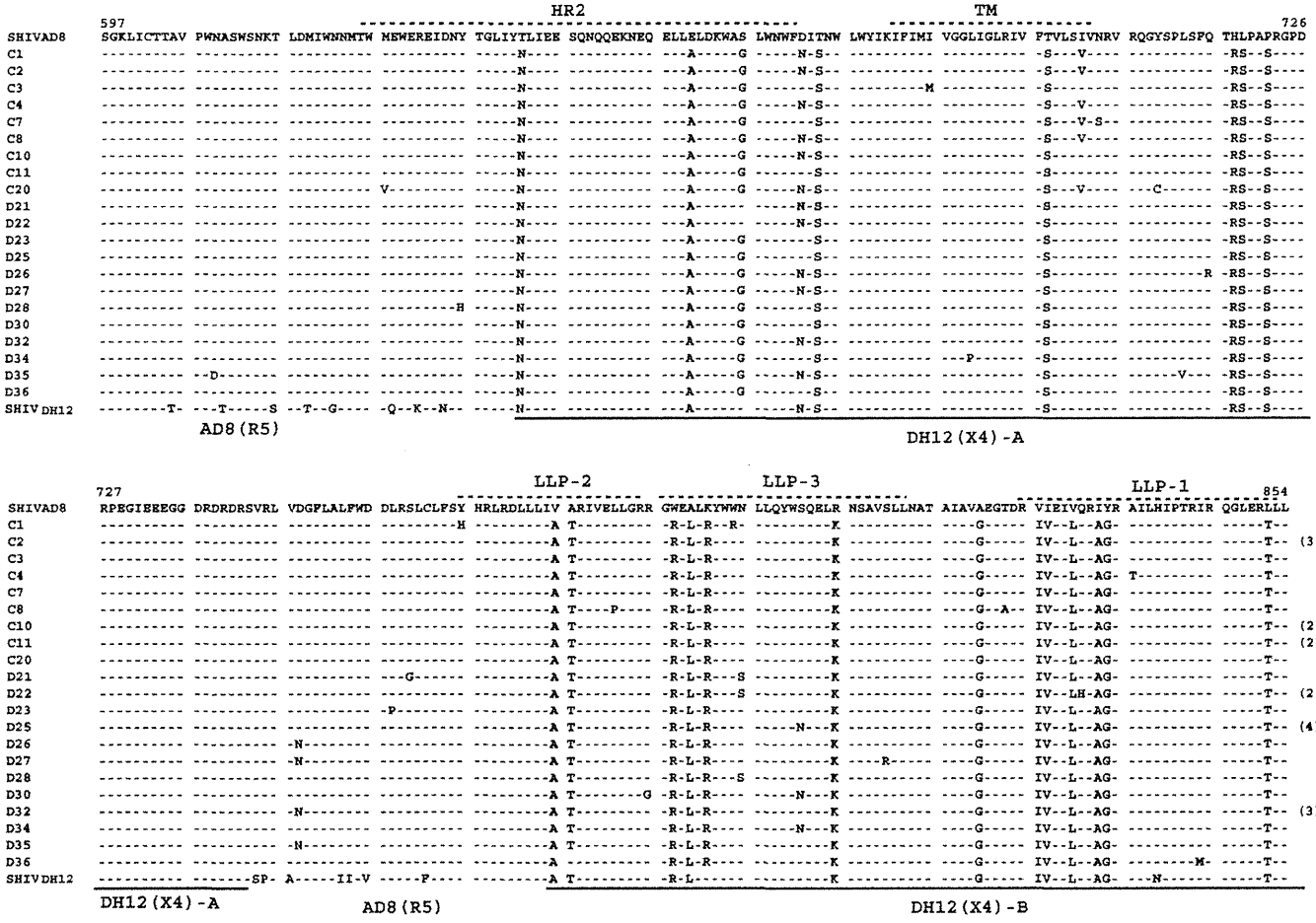

FIG. 4. Two regions of the input X4 SHIV gp41 *env* gene region have been transferred by intergenomic recombination into the genetic background of $SHIV_{AD8}$. SGA and direct sequencing of gp41 *env* sequences present in plasma viral RNA at week 100 p.i. are shown. The gp41 sequences in the input $SHIV_{AD8}$ and $SHIV_{DH12}$ are presented in the top and bottom lines, respectively. The heptad repeat 2 (HR2), transmembrane (TM), and lentivirus lytic peptide (LLP) regions are annotated at the top. The origin of the gp41 sequences are indicated at the bottom.

amplicons (18/18) generated at this time contained the two gp41 segments from the starting X4 SHIV, embedded into the R5-SHIV *env* gene, as previously seen in the week 100 plasma sample (Fig. 3). The remainder of the original R5-tropic *env* gene present in the week 31 SHIV remained essentially unchanged from that present in the starting inoculum. Interestingly, the recombination events involving the gp41 gene segment had eliminated the target sequences used to amplify the starting R5-tropic SHIV, explaining our inability to detect this virus with isolate-specific gp41 primer pairs after week 20 p.i. All amplicons of the week 31 plasma virus also contained a previously unrecognized 147-nt segment containing overlapping *tat*, *rev*, and *vpu* gene sequences (Fig. 7) from the input X4-tropic SHIV, which had been inserted into the genetic background of the R5-tropic SHIV (Fig. 6). No amplicons representing the original X4-tropic SHIV *env* gene were detectable in plasma at week 31 p.i. by SGA.

At week 64 p.i., SGA revealed the presence of two circulating viral populations (Fig. 6). One was indistinguishable from the single circulating R5 virus species identified at week 31. The second virus population at week 64 p.i. (56% of the amplicons) carried the V3 region from the starting X4-tropic SHIV embedded into the genetic background of the R5 *env* gene. A similar ratio of the two SHIV species persisted in the plasma from week 64 to the time of euthanasia at week 100. Taken together, these results suggested that the rapid loss of $CD4^+$ T cells accompanying the increased plasma virus loads in macaque CE43 after week 51 was associated with recombination-mediated coreceptor switching that introduced novel CXCR4 entry determinants into the circulating monophyletic R5-tropic virus.

The emergence of the X4 V3 recombinant SHIV at week 64 p.i. raised the possibility that the earlier *tat*, *rev*, or *vpu* gene and gp41 recombinant virus might have been a necessary intermediate because it conferred augmented replicative properties that facilitated recombination. This was evaluated by infecting rhesus monkey PBMC with the original $SHIV_{AD8}$ and recombinant SHIVs containing the *tat*, *rev*, and *vpu* gene and gp41 inserts with (designated $SHIV_{AD8\text{-}ES3N6}$) or without (designated $SHIV_{AD8\text{-}ES3T7}$) the V3 sequences. As shown in Fig. 8, the SHIV carrying only the *tat*, *rev*, and *vpu* gene plus gp41 inserts exhibited robust infectivity in macaque PBMC compared to the original $SHIV_{AD8}$. The addition of V3 sequences to this recombinant greatly acceler-

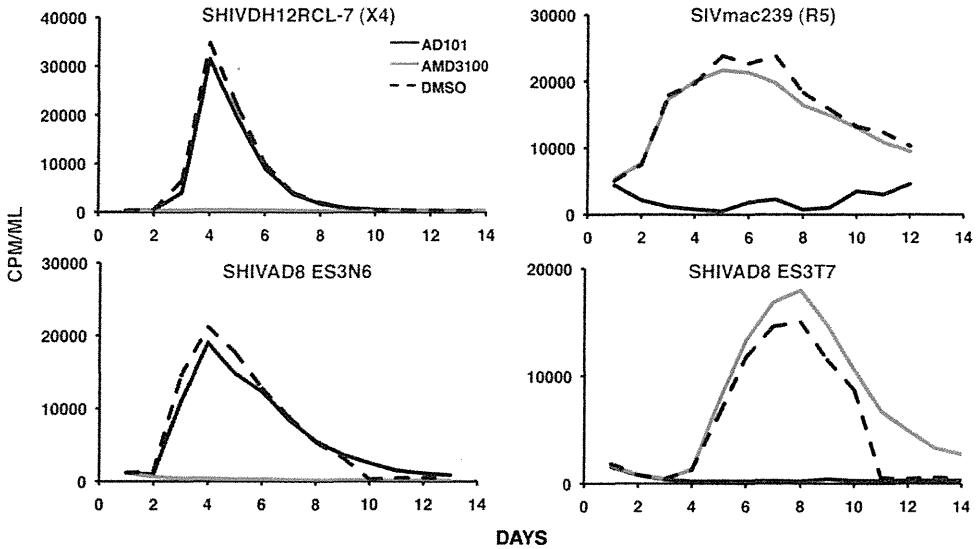

FIG. 5. Coreceptor utilization by SHIVs containing recombinant *env* genes. The indicated viruses were spinoculated onto rhesus PBMC in the presence of CCR5 (AD101)- or CXCR4 (AMD3100)-specific inhibitors. Particle-associated reverse transcriptase activity released into the medium during a 14-day infection was measured in the presence or absence (dashed lined) of inhibitor.

ated virus production in PBMC. Taken together, these results suggest that the week 31 SHIV recombinant may be more fit *in vivo*, than the input R5 SHIV. Thus the incorporation of the *tat*, *rev*, and *vpu* gene plus gp41 sequences may have facilitated the subsequent coinfection of $CD4^+$ T cells and resulted in the generation of the week 64 recombinant X4 SHIV.

X4 SHIV proviral DNA was detectable in PBMC but not as cell-free virus in the blood of macaque CE43. The SGA anal-

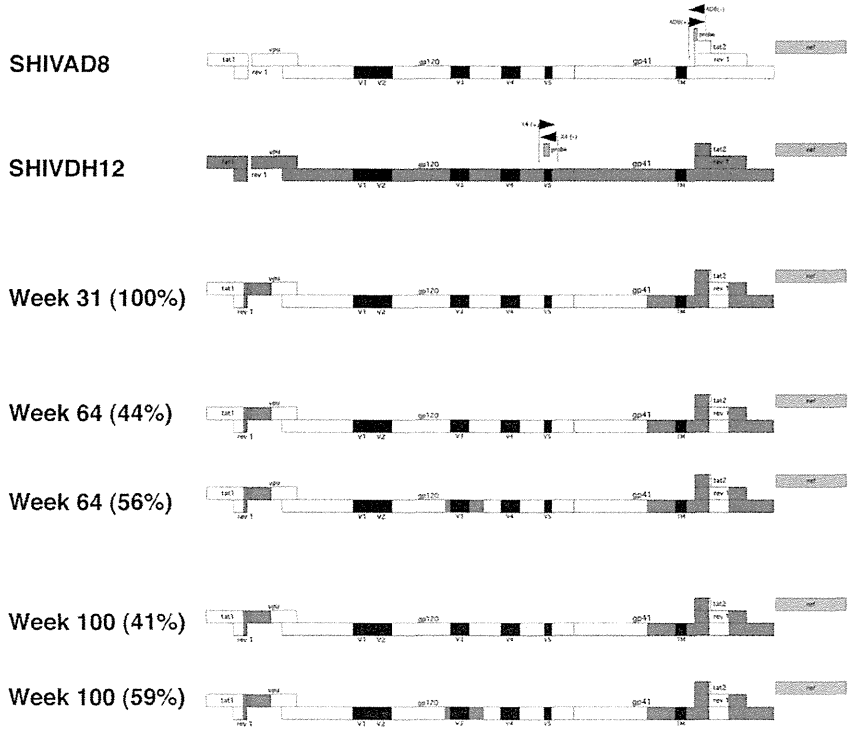

FIG. 6. Time line of recombination events occurring in macaque CE43 following the inoculation of X4 and R5 SHIVs. Sequences present in the starting R5-tropic $SHIV_{AD8}$ are indicated in white, and those from the X4-tropic $SHIV_{DH12}$ are indicated in red. The black rectangles denote HIV-1 gp120 variable regions, and the yellow bar denotes the SIVmac239 *nef* gene. The locations of primer pairs and probe sequences used to detect the R5 and X4 SHIVs are indicated by the pair of opposing arrows. The numbers in parentheses represent the percentage of each recombinant at the indicated times, as determined by SGA. Note that the recombination-mediated insertion of gp41 sequences from SHIVDH12 into SHIVAD8 at week 31 eliminated sequences used for detecting the starting R5 SHIVAD8.

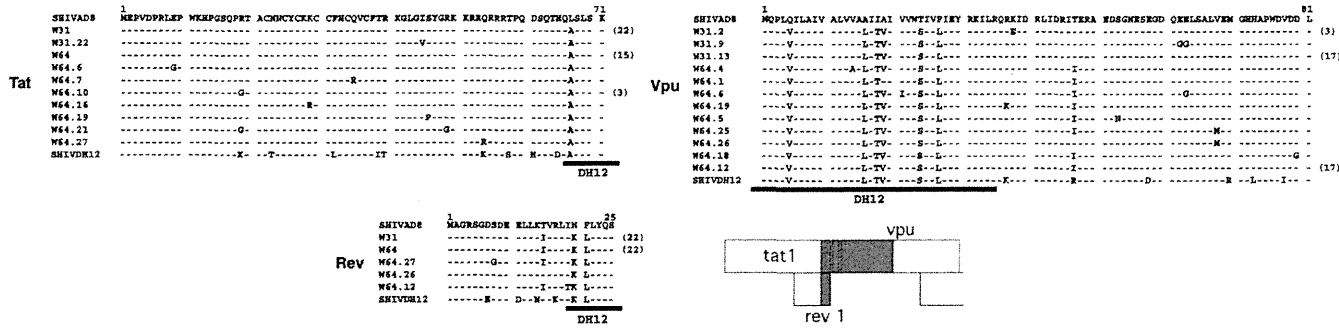

FIG. 7. A short gene segment containing overlapping *tat* and *rev* and adjacent *vpu* sequences was transferred from the input X4 SHIVDH12 into R5 SHIVAD8 by intergenomic recombination. SGA and direct sequencing of plasma samples collected at weeks 31 and 64 p.i. were used to generate amplicons containing the first exons of the *tat*, *rev*, and *vpu* genes shown. The black bars below each sequence indicate the region contributed by the starting X4-tropic SHIVDH12. The numbers in parentheses denote the amplicons with the indicated sequence.

yses reported above indicated that after week 20 p.i., the predominant viruses circulating in plasma were derivatives of the starting R5 SHIV into which segments of the original X4 SHIV have been additively inserted. The absence of detectable X4 SHIV RNA in the plasma after week 10 prompted us to examine infected cells for the presence of the input X4 SHIV provirus. Since lymph node specimens were not available, preserved PBMC were analyzed by real-time DNA PCR, using the same primers and probe previously used in real-time RT-PCRs for detection of the starting X4-tropic SHIV RNA in plasma. As shown in Fig. 9, the cell-associated X4 SHIV DNA peaked at 334 copies/10^5 PBMC at week 3 p.i. and then gradually declined over the next 12 months. At week 27 p.i., just prior to the emergence of the *tat*, *rev*, and *vpu* gene and gp41 recombinants, the frequency of cell-associated X4 SHIV DNA was 53 copies/10^5 PBMC. The detection of cell-associated X4 SHIV proviral DNA in circulating PBMC suggested that low levels of virus-infected $CD4^+$ T cells were present in some body compartment of macaque CE43, most likely secondary lymphoid tissues.

Immune responses directed against the starting and recombinant SHIVs in macaque CE43. Antiviral SIV Gag-specific (present in both X4 and R5 SHIVs) cytotoxic T lymphocyte responses were measured by flow cytometry by intracellular staining for tumor necrosis factor alpha and or gamma interferon at weeks 19, 35, and 43 p.i. The levels of anti-Gag specific $CD8^+$ T cells at these times were 0, 3.1, and 3.6%, respectively, indicating that a strong antiviral cell-mediated response had been elicited during the first year of the dual SHIV infection.

Antiviral NAbs directed against the starting X4 and R5 SHIVs were also assessed. A 1:20 dilution of plasma samples, collected at different times throughout the 100-week infection of macaque CE43, was used in the TZM-bl cell assay system to determine the presence of neutralization activity against each virus. As shown in Fig. 10, high levels of NAbs directed against the starting X4-tropic $SHIV_{DH12}$ were detected by week 8 and peaked at week 14 p.i. This result is consistent with previous reports from our laboratory, using a different virus neutralization assay system, showing that X4 $SHIV_{DH12}$ derivatives generate NAbs between weeks 4 and 10 p.i. (10, 20). A limiting dilution assay indicated a 50% neutralization titer of 1:121 against the input X4 $SHIV_{DH12}$ at week 14 p.i. After week 45 p.i., the levels of NAb activity against the starting $SHIV_{DH12}$, measured at a 1:20 dilution of plasma, had declined to near background levels (<30% neutralization).

We recently reported that NAbs directed against $SHIV_{AD8}$ became detectable after week 25 p.i. in some infected rhesus monkeys, and the titers measured correlated with the levels of

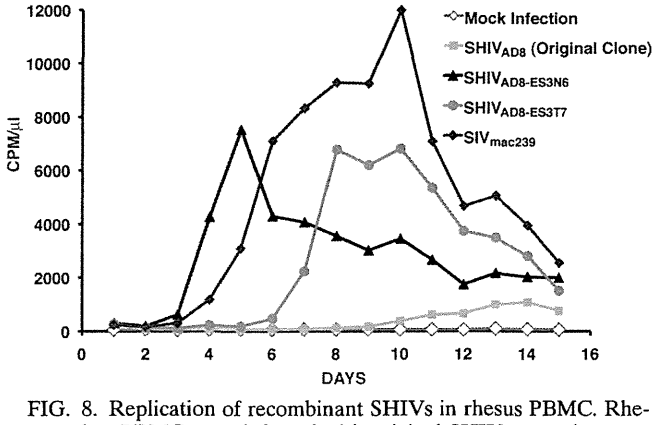

FIG. 8. Replication of recombinant SHIVs in rhesus PBMC. Rhesus monkey PBMC were infected with original $SHIV_{AD8}$ and recombinant SHIVs containing the *tat*, *rev*, or *vpu* gene and gp41 inserts with ($SHIV_{AD8\text{-}ES3N6}$) or without ($SHIV_{AD8\text{-}ES3T7}$) the V3 sequences, normalized for RT activity. Virus production was monitored by RT activity released into the medium.

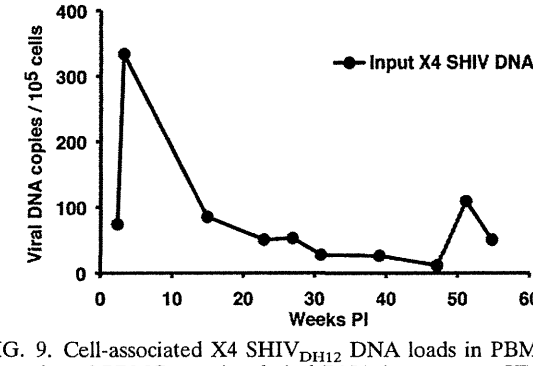

FIG. 9. Cell-associated X4 $SHIV_{DH12}$ DNA loads in PBMC. The frequencies of PBMC-associated viral DNA in macaque CE43 were determined over a 55-week period by quantitative real-time PCR using the primers and probe specifically detecting the starting X4 $SHIV_{DH12}$ *env* gene.

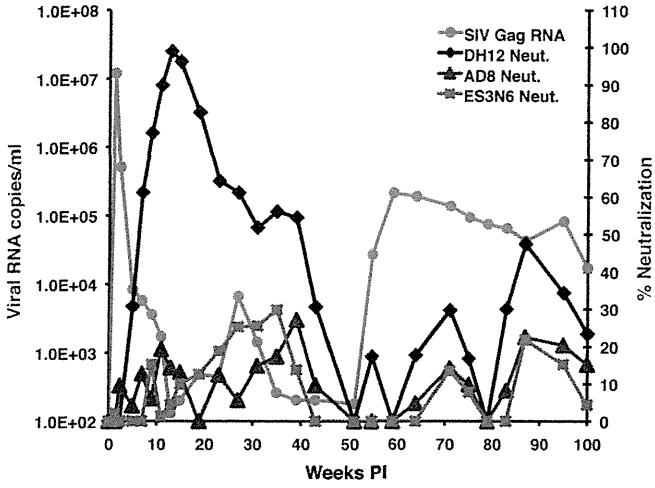

FIG. 10. Neutralizing antibodies are directed against the input X4 SHIVDH12 but not against the recombinant X4 SHIV that emerged in macaque CE43. Plasma samples (1:20 dilution) were collected from dually infected animal CE43 at the indicated times, incubated with the input X4 $SHIV_{DH12}$, the input $SHIV_{AD8}$, or the recombinant X4 $SHIV_{ES3N6}$ for 1 h at 37°C, and assayed for infectivity in TZM-bl cells. Plasma viral RNA levels were determined by using *gag* gene primer pairs and probes.

set point viremia (34). In general, anti-$SHIV_{AD8}$ NAbs were not detected when plasma viral loads were lower than 10^3 RNA copies/ml. As shown in Fig. 8, NAbs directed against the starting R5 $SHIV_{AD8}$ were never detected during the 100-week observation period, even when plasma viremia exceeded 10^5 RNA copies/ml at week 59 p.i. The TZM-bl cell assay system was also used to monitor any NAb activity directed against the recombinant X4 SHIV, which emerged at week 51 p.i. As represented by the reconstructed $SHIV_{AD8\text{-}ES3N6}$, which exclusively uses CXCR4 to enter rhesus PBMC, no NAbs were detected during the entire course of infection in macaque CE43. These results suggest that both cell-mediated and humoral immune responses potently and durably suppressed the input X4 SHIV, which became undetectable by RT-PCR in plasma after week 10 p.i. On the other hand, the late-emerging recombinant X4 SHIV elicited no NAbs, due to either continued masking of envelope glycoprotein epitopes (derived primarily from the original R5 SHIV) or to irreversible damage to the immune system accompanying the rapid depletion of $CD4^+$ T cells after week 70 p.i.

DISCUSSION

Coreceptor switching has rarely been reported during pathogenic SIV infections of rhesus macaques, although a molecular clone (SIVmac155/T3), carrying the *env* gene recovered from the tissues of an infected monkey, has been constructed, which uses CXCR4 in cell entry assays and causes the depletion of naive $CD4^+$ T lymphocytes in inoculated rhesus macaques (37). In contrast, coreceptor switching has been reported in rhesus monkeys infected with R5 SHIVs. Cheng-Mayer and coworkers have described the emergence of dualtropic or X4-tropic SHIVs in four rapid progressors following inoculations of $SHIV_{SF162P3}$ derivatives (12, 13, 42). We previously reported that one of three R5 $SHIV_{AD8}$ rapid progressors had experienced coreceptor switching (34). In all of these animals, coreceptor switching occurred within months of virus inoculation rather than during the late symptomatic phase of infection as reported for HIV-1.

The overwhelming evidence accumulated over more than 2 decades of HIV-1 natural history studies points to the evolution of a transmitted R5-tropic *env* gene, particularly its V3 loop, as the driving force for coreceptor switching in chronically infected individuals. Numerous reports have identified R5 HIV-1 strains, but not X4 viruses, in plasma following seroconversion or during the asymptomatic phase of the *in vivo* infection. The X4 virus that emerges during the late stages of the HIV-1 infection usually bears an *env* gene, which is genetically related to the homologue present in the coexisting R5 strain except for changes in the V3 region. These results are consistent with SGA analyses that have identified only one or two transmitted virus species in plasma of recently HIV-1-infected individuals, the vast majority of which were R5-tropic (23, 47, 49).

It is still possible that the reemergence of cotransmitted X4-tropic HIV-1 strains may contribute to coreceptor switching in some infected individuals. SGA analyses performed to date have only evaluated virus strains circulating in the blood during the acute infection and not in tissues such as the gut-associated lymphoid tissues and draining lymph nodes, the primary site of virus replication during the acute infection. A recent clonal analysis of HIV-1 present in 150 recent seroconverters revealed that CXCR4 using viruses, validated in cell entry assays, were present in seven individuals (15). Even if the establishment of dual X4 and R5 HIV-1 infections occurs at low frequencies in recently exposed individuals, the generation of dualtropic/X4 strains by substitutional evolution of the input R5 virus can occur at anytime following virus acquisition. The SHIV/macaque system described here could therefore also model the intrapatient recombination between R5 HIV-1 *env* gene NAb escape variants and suppressed X4 HIV strains, which emerged postacquisition. An X4 HIV-1 recombinant arising from such an event might be able to change its neutralization phenotype and target both naive and memory $CD4^+$ T lymphocytes *in vivo*, thereby further compromising the immune system. In this regard, several studies, published since 2005, have reported a high prevalence of circulating dualtropic or X4-tropic viral strains (50% or greater) in heavily treatment experienced HIV-1-infected patients (9, 16, 56) compared to antiretroviral naive individuals (18 to 19%) (3, 29). In one of these studies, 11 of 23 patients on highly active antiretroviral therapy (HAART) for 5 years with undetectable levels of viral RNA experienced a switch from R5 (at baseline) to X4-tropic strains (9). It is currently unclear why HAART suppression of HIV-1 replication unmasks preexisting CXCR4 utilizing virus strains. Taken together, these studies suggest that previously unrecognized X4 HIV-1 variants may be present throughout the infection.

Our results demonstrate that the potential consequences of recombination *in vivo* may be functionally profound. Retrovirus recombination is predicated on the dual infection of a single cell by two viruses, the copackaging of nonhomologous genomic RNAs into progeny particles, and template switching during subsequent rounds of reverse transcription. For HIV-1,

recombination events have given rise to circulating recombinant forms (45), augmented the spread of resistance to antiretroviral drugs (35), and accelerated disease progression (26). Although we have described recombination between X4 and R5 *env* gene segments in a single dually infected animal, several studies have reported X4 and R5 intrapatient recombination events in HIV-1-infected individuals (4, 24, 54). Moreover, a recent study examining the genotype and coreceptor usage of clones derived from sequential isolates from four patients experiencing coreceptor switching determined that (i) 9% of clones using the CXCR4 receptor arose by recombination and (ii) a majority of breakpoints identified were located in the gp120 C2 region and involved the transfer of the V3 region of gp120 (28).

In the present study, the recombination events observed in macaque CE43 were multistep and invariably unidirectional (transfer of gene segments from the input X4 SHIV into the genetic background of the starting R5-tropic SHIV). Based on coreceptor usage, a plausible scenario to explain our results would involve a SHIV coinfection of memory $CD4^+$ T lymphocytes, which, unlike the naive $CD4^+$ subset, are susceptible to both X4 and R5 SHIVs. The transfers of *tat*, *rev*, or *vpu* and gp41 gene segments from the X4 SHIV into the genetic background of the starting R5 SHIV between weeks 15 and 31 p.i. were the first recombination events identified (Fig. 6). Infectivity analyses carried out in rhesus monkey PBMC demonstrated that these early recombinations greatly improved the replication capacity of the input R5 SHIV and was reflected by a transient increase of set-point viremia during this phase of the infection.

The subsequent transfer of the gp120 V3 region from the X4-tropic SHIV parent to the monophyletic recombinant R5 SHIV circulating at week 50 p.i. greatly increased plasma viremia and irreversibly altered the clinical course. This second phase of recombination created a virus with two novel properties: (i) the capacity of infect both memory and naive $CD4^+$ T lymphocytes and (ii) a neutralization-resistant X4-tropic gp120. In contrast to the starting X4 SHIV, which possessed neutralization epitopes mapping to the V1/V2 and V4 regions of gp120 (5), the novel recombinant X4 SHIV that emerged had acquired the neutralization resistant properties of the input R5 SHIV (Fig. 10). The unidirectionality of the recombinations described (X4 SHIV to R5 SHIV) were all stochastic events, very likely driven by the prior *in vivo* passaging of the X4-tropic $SHIV_{DH12}$ that optimized replication in macaques (19), as well as the NAb sensitivities of the starting X4 and R5 SHIVs. The products of these recombinations (a nearly 50/50% mixture of recombinant X4 and R5 SHIVs, each possessing robust replication properties) were highly virulent, accelerating progression to AIDS in macaque CE43 and causing an extraordinarily rapid depletion of $CD4^+$ T cells following intravenous transfer to two recipient animals.

ACKNOWLEDGMENTS

We thank Robin Kruthers and Ronald Plishka for nucleotide sequence analyses determining viral RNA levels and Vanessa Hirsch for critical comments during preparation of the manuscript. We thank Boris Skopits, Amy Fuse, and Rahel Petros for diligently assisting in the care and maintenance of our animals. We are indebted to the NIH AIDS Research and Reference Reagent Program for providing AMD3100 and to Julie Strizki, Shering Plough, for providing AD101.

This study was supported by the Intramural Research Program of the National Institute of Allergy and Infectious Diseases, National Institutes of Health.

REFERENCES

1. **Berger, E. A., P. M. Murphy, and J. M. Farber.** 1999. Chemokine receptors as HIV-1 coreceptors: roles in viral entry, tropism, and disease. Annu. Rev. Immunol. **17**:657–700.
2. **Brown, C. R., et al.** 2007. Unique pathology in simian immunodeficiency virus-infected rapid progressor macaques is consistent with a pathogenesis distinct from that of classical AIDS. J. Virol. **81**:5594–5606.
3. **Brumme, Z. L., et al.** 2005. Molecular and clinical epidemiology of CXCR4-using HIV-1 in a large population of antiretroviral-naive individuals. J. Infect. Dis. **192**:466–474.
4. **Charpentier, C., T. Nora, O. Tenaillon, F. Clavel, and A. J. Hance.** 2006. Extensive recombination among human immunodeficiency virus type 1 quasispecies makes an important contribution to viral diversity in individual patients. J. Virol. **80**:2472–2482.
5. **Cho, M. W., M. K. Lee, C. H. Chen, T. Matthews, and M. A. Martin.** 2000. Identification of gp120 regions targeted by a highly potent neutralizing antiserum elicited in a chimpanzee inoculated with a primary human immunodeficiency virus type 1 isolate. J. Virol. **74**:9749–9754.
6. **Connor, R. I., K. E. Sheridan, D. Ceradini, S. Choe, and N. R. Landau.** 1997. Change in coreceptor use correlates with disease progression in HIV-1-infected individuals. J. Exp. Med. **185**:621–628.
7. **Dean, M., et al.** 1996. Genetic restriction of HIV-1 infection and progression to AIDS by a deletion allele of the CKR5 structural gene. Science **273**:1856–1862.
8. **De Jong, J. J., A. De Ronde, W. Keulen, M. Tersmette, and J. Goudsmit.** 1992. Minimal requirements for the human immunodeficiency virus type 1 V3 domain to support the syncytium-inducing phenotype: analysis by single amino acid substitution. J. Virol. **66**:6777–6780.
9. **Delobel, P., et al.** 2005. R5 to X4 switch of the predominant HIV-1 population in cellular reservoirs during effective highly active antiretroviral therapy. J. Acquir. Immune Defic. Syndr. **38**:382–392.
10. **Endo, Y., et al.** 2000. Short- and long-term clinical outcomes in rhesus monkeys inoculated with a highly pathogenic chimeric simian/human immunodeficiency virus. J. Virol. **74**:6935–6945.
11. **Fouchier, R. A., et al.** 1992. Phenotype-associated sequence variation in the third variable domain of the human immunodeficiency virus type 1 gp120 molecule. J. Virol. **66**:3183–3187.
12. **Ho, S. H., et al.** 2007. Coreceptor switch in R5-tropic simian/human immunodeficiency virus-infected macaques. J. Virol. **81**:8621–8633.
13. **Ho, S. H., N. Trunova, A. Gettie, J. Blanchard, and C. Cheng-Mayer.** 2008. Different mutational pathways to CXCR4 coreceptor switch of CCR5-using simian-human immunodeficiency virus. J. Virol. **82**:5653–5656.
14. **Huang, W., et al.** 2008. Coreceptor tropism can be influenced by amino acid substitutions in the gp41 transmembrane subunit of human immunodeficiency virus type 1 envelope protein. J. Virol. **82**:5584–5593.
15. **Huang, W., et al.** 2009. Characterization of human immunodeficiency virus type 1 populations containing CXCR4-using variants from recently infected individuals. AIDS Res. Hum. Retrovir. **25**:795–802.
16. **Hunt, P. W., et al.** 2006. Prevalence of CXCR4 tropism among antiretroviral-treated HIV-1-infected patients with detectable viremia. J. Infect. Dis. **194**: 926–930.
17. **Igarashi, T., et al.** 2003. Macrophage-tropic simian/human immunodeficiency virus chimeras use CXCR4, not CCR5, for infections of rhesus macaque peripheral blood mononuclear cells and alveolar macrophages. J. Virol. **77**:13042–13052.
18. **Igarashi, T., et al.** 2007. Although macrophage-tropic simian/human immunodeficiency viruses can exhibit a range of pathogenic phenotypes, a majority of isolates induce no clinical disease in immunocompetent macaques. J. Virol. **81**:10669–10679.
19. **Igarashi, T., et al.** 1999. Emergence of a highly pathogenic simian/human immunodeficiency virus in a rhesus macaque treated with anti-CD8 MAb during a primary infection with a nonpathogenic virus. Proc. Natl. Acad. Sci. U. S. A. **96**:14049–14054.
20. **Igarashi, T., et al.** 2003. Early control of highly pathogenic simian immunodeficiency virus/human immunodeficiency virus chimeric virus infections in rhesus monkeys usually results in long-lasting asymptomatic clinical outcomes. J. Virol. **77**:10829–10840.
21. **Jensen, M. A., et al.** 2003. Improved coreceptor usage prediction and genotypic monitoring of R5-to-X4 transition by motif analysis of human immunodeficiency virus type 1 env V3 loop sequences. J. Virol. **77**:13376–13388.
22. **Karlsson, A., K. Parsmyr, E. Sandstrom, E. M. Fenyo, and J. Albert.** 1994. MT-2 cell tropism as prognostic marker for disease progression in human immunodeficiency virus type 1 infection. J. Clin. Microbiol. **32**:364–370.
23. **Keele, B. F., et al.** 2008. Identification and characterization of transmitted and early founder virus envelopes in primary HIV-1 infection. Proc. Natl. Acad. Sci. U. S. A. **105**:7552–7557.
24. **Kemal, K. S., et al.** 2003. HIV-1 in genital tract and plasma of women:

compartmentalization of viral sequences, coreceptor usage, and glycosylation. Proc. Natl. Acad. Sci. U. S. A. **100:**12972–12977.
25. **Kirchhoff, F., et al.** 1997. Simian immunodeficiency virus variants with differential T-cell and macrophage tropism use CCR5 and an unidentified cofactor expressed in CEMx174 cells for efficient entry. J. Virol. **71:**6509–6516.
26. **Liu, S. L., et al.** 2002. Selection for human immunodeficiency virus type 1 recombinants in a patient with rapid progression to AIDS. J. Virol. **76:** 10674–10684.
27. **Margulies, B. J., D. A. Hauer, and J. E. Clements.** 2001. Identification and comparison of eleven rhesus macaque chemokine receptors. AIDS Res. Hum. Retrovir. **17:**981–986.
28. **Mild, M., J. Esbjornsson, E. M. Fenyo, and P. Medstrand.** 2007. Frequent intrapatient recombination between human immunodeficiency virus type 1 R5 and X4 envelopes: implications for coreceptor switch. J. Virol. **81:**3369–3376.
29. **Moyle, G. J., et al.** 2005. Epidemiology and predictive factors for chemokine receptor use in HIV-1 infection. J. Infect. Dis. **191:**866–872.
30. **National Institutes of Health.** 1985. Guide for the care and use of laboratory animals. Department of Health and Human Services publication no. NIH 85-23. National Institutes of Health, Bethesda, MD.
31. **Nishimura, Y., et al.** 2005. Resting naive $CD4^+$ T cells are massively infected and eliminated by X4-tropic simian-human immunodeficiency viruses in macaques. Proc. Natl. Acad. Sci. U. S. A. **102:**8000–8005.
32. **Nishimura, Y., et al.** 2007. Loss of naive cells accompanies memory $CD4^+$ T-cell depletion during long-term progression to AIDS in simian immunodeficiency virus-infected macaques. J. Virol. **81:**893–902.
33. **Nishimura, Y., et al.** 2004. Highly pathogenic SHIVs and SIVs target different $CD4^+$ T cell subsets in rhesus monkeys, explaining their divergent clinical courses. Proc. Natl. Acad. Sci. U. S. A. **101:**12324–12329.
34. **Nishimura, Y., et al.** 2010. Generation of the pathogenic R5-tropic simian/human immunodeficiency virus SHIVAD8 by serial passaging in rhesus macaques. J. Virol. **84:**4769–4781.
35. **Nora, T., et al.** 2007. Contribution of recombination to the evolution of human immunodeficiency viruses expressing resistance to antiretroviral treatment. J. Virol. **81:**7620–7628.
36. **O'Doherty, U., W. J. Swiggard, and M. H. Malim.** 2000. Human immunodeficiency virus type 1 spinoculation enhances infection through virus binding. J. Virol. **74:**10074–10080.
37. **Picker, L. J., et al.** 2004. Insufficient production and tissue delivery of $CD4^+$ memory T cells in rapidly progressive simian immunodeficiency virus infection. J. Exp. Med. **200:**1299–1314.
38. **Pitcher, C. J., et al.** 2002. Development and homeostasis of T cell memory in rhesus macaque. J. Immunol. **168:**29–43.
39. **Pollakis, G., et al.** 2001. N-linked glycosylation of the HIV type-1 gp120 envelope glycoprotein as a major determinant of CCR5 and CXCR4 coreceptor utilization. J. Biol. Chem. **276:**13433–13441.
40. **Regoes, R. R., and S. Bonhoeffer.** 2005. The HIV coreceptor switch: a population dynamical perspective. Trends Microbiol. **13:**269–277.
41. **Reimann, K. A., et al.** 1996. A chimeric simian/human immunodeficiency virus expressing a primary patient human immunodeficiency virus type 1 isolate *env* causes an AIDS-like disease after in vivo passage in rhesus monkeys. J. Virol. **70:**6922–6928.
42. **Ren, W., et al.** 2010. Different tempo and anatomic location of dualtropic and X4 virus emergence in a model of R5 simian-human immunodeficiency virus infection. J. Virol. **84:**340–351.
43. **Resch, W., N. Hoffman, and R. Swanstrom.** 2001. Improved success of phenotype prediction of the human immunodeficiency virus type 1 from envelope variable loop 3 sequence using neural networks. Virology **288:** 51–62.
44. **Richman, D. D., and S. A. Bozzette.** 1994. The impact of the syncytium-inducing phenotype of human immunodeficiency virus on disease progression. J. Infect. Dis. **169:**968–974.
45. **Robertson, D. L., et al.** 2000. HIV-1 nomenclature proposal. Science **288:** 55–56.
46. **Sadjadpour, R., et al.** 2004. Induction of disease by a molecularly cloned highly pathogenic simian immunodeficiency virus/human immunodeficiency virus chimera is multigenic. J. Virol. **78:**5513–5519.
47. **Sagar, M., et al.** 2009. Selection of HIV variants with signature genotypic characteristics during heterosexual transmission. J. Infect. Dis. **199:**580–589.
48. **Salazar-Gonzalez, J. F., et al.** 2008. Deciphering human immunodeficiency virus type 1 transmission and early envelope diversification by single-genome amplification and sequencing. J. Virol. **82:**3952–3970.
49. **Salazar-Gonzalez, J. F., et al.** 2009. Genetic identity, biological phenotype, and evolutionary pathways of transmitted/founder viruses in acute and early HIV-1 infection. J. Exp. Med. **206:**1273–1289.
50. **Samson, M., et al.** 1996. Resistance to HIV-1 infection in Caucasian individuals bearing mutant alleles of the CCR-5 chemokine receptor gene. Nature **382:**722–725.
51. **Schuitemaker, H., et al.** 1992. Biological phenotype of human immunodeficiency virus type 1 clones at different stages of infection: progression of disease is associated with a shift from monocytotropic to T-cell-tropic virus population. J. Virol. **66:**1354–1360.
52. **Shibata, R., et al.** 1997. Infection and pathogenicity of chimeric simian-human immunodeficiency viruses in macaques: determinants of high virus loads and CD4 cell killing. J. Infect. Dis. **176:**362–373.
53. **Tersmette, M., and F. Miedema.** 1990. Interactions between HIV and the host immune system in the pathogenesis of AIDS. AIDS **4**(Suppl. 1)**:**S57–S66.
54. **van Rij, R. P., M. Worobey, J. A. Visser, and H. Schuitemaker.** 2003. Evolution of R5 and X4 human immunodeficiency virus type 1 *gag* sequences in vivo: evidence for recombination. Virology **314:**451–459.
55. **van't Wout, A. B., et al.** 1994. Macrophage-tropic variants initiate human immunodeficiency virus type 1 infection after sexual, parenteral, and vertical transmission. J. Clin. Invest. **94:**2060–2067.
56. **Wilkin, T. J., et al.** 2007. HIV type 1 chemokine coreceptor use among antiretroviral-experienced patients screened for a clinical trial of a CCR5 inhibitor: AIDS Clinical Trial Group A5211. Clin. Infect. Dis. **44:**591–595.
57. **Willey, R., M. C. Nason, Y. Nishimura, D. A. Follmann, and M. A. Martin.** Neutralizing antibody titers conferring protection to macaques from a simian/human immunodeficiency virus challenge using the TZM-bl assay. AIDS Res. Hum. Retrovir. **26:**89–98.
58. **Willey, R. L., et al.** 1988. In vitro mutagenesis identifies a region within the envelope gene of the human immunodeficiency virus that is critical for infectivity. J. Virol. **62:**139–147.
59. **Zhang, Y., et al.** 2000. Use of inhibitors to evaluate coreceptor usage by simian and simian/human immunodeficiency viruses and human immunodeficiency virus type 2 in primary cells. J. Virol. **74:**6893–6910.
60. **Zhu, T., et al.** 1993. Genotypic and phenotypic characterization of HIV-1 patients with primary infection. Science **261:**1179–1181.

Microbiology and Immunology

Microbiol Immunol 2011; **55**: 768–773
doi:10.1111/j.1348-0421.2011.00384.x

ORIGINAL ARTICLE

Major histocompatibility complex class I-restricted cytotoxic T lymphocyte responses during primary simian immunodeficiency virus infection in Burmese rhesus macaques

Midori Nakamura[1,2], Yusuke Takahara[1,2], Hiroshi Ishii[1,2], Hiromi Sakawaki[3], Mariko Horiike[3], Tomoyuki Miura[3], Tatsuhiko Igarashi[3], Taeko K. Naruse[4], Akinori Kimura[4], Tetsuro Matano[1,2] and Saori Matsuoka[2]

[1]Division for AIDS Vaccine Development, Institute of Medical Science, University of Tokyo, 4-6-1 Shirokanedai, Minato-ku, Tokyo 108-8639, [2]AIDS Research Center, National Institute of Infectious Diseases, 1-23-1 Toyama, Shinjuku-ku, Tokyo 162-8640, [3]Institute for Virus Research, Kyoto University, 53 Kawahara-cho, Shogoin, Sakyo-ku, Kyoto 606-8507, and [4]Department of Molecular Pathogenesis, Medical Research Institute, Tokyo Medical and Dental University, 2-3-10 Kandasurugadai, Chiyoda-ku, Tokyo 101-0062, Japan

ABSTRACT

Major histocompatibility complex class I (MHC-I)-restricted CD8$^+$ cytotoxic T lymphocyte (CTL) responses are crucial for the control of human immunodeficiency virus (HIV) and simian immunodeficiency virus (SIV) replication. In particular, Gag-specific CTL responses have been shown to exert strong suppressive pressure on HIV/SIV replication. Additionally, association of Vif-specific CTL frequencies with *in vitro* anti-SIV efficacy has been suggested recently. Host MHC-I genotypes could affect the immunodominance patterns of these potent CTL responses. Here, Gag- and Vif-specific CTL responses during primary SIVmac239 infection were examined in three groups of Burmese rhesus macaques, each group having a different MHC-I haplotype. The first group of four macaques, which possessed the MHC-I haplotype *90-010-Ie*, did not show Gag- or Vif-specific CTL responses. However, Nef-specific CTL responses were elicited, suggesting that primary SIV infection does not induce predominant CTL responses specific for Gag/Vif epitopes restricted by *90-010-Ie*-derived MHC-I molecules. In contrast, Gag- and Vif-specific CTL responses were induced in the second group of two *89-075-Iw*-positive animals and the third group of two *91-010-Is*-positive animals. Considering the potential of prophylactic vaccination to affect CTL immunodominance post-viral exposure, these groups of macaques would be useful for evaluation of vaccine antigen-specific CTL efficacy against SIV infection.

Key words cytotoxic T lymphocyte, human immunodeficiency virus, major histocompatibility complex, simian immunodeficiency virus.

Virus-specific CD8$^+$ CTL responses are crucial for the control of HIV and SIV replication (1–5). CTLs recognize specific epitopes which are presented on the target cell surface by binding to the MHC-I molecule. There have been many reports indicating association of MHC-I (HLA class I) genotypes with rapid or delayed AIDS progression in HIV-infected people (6–8). For instance, most of the HIV-infected individuals possessing *HLA-B*57* have a better prognosis and smaller viral loads, implicating HLA-B*57-restricted epitope-specific CTL responses in control

Correspondence
Saori Matsuoka, AIDS Research Center, National Institute of Infectious Diseases, 1-23-1 Toyama, Shinjuku-ku, Tokyo 162-8640, Japan.
Tel: 81 3 5285 1111; Fax: 81 3 5285 1165; e-mail: s-matsu@nih.go.jp

Received 11 May 2011; revised 18 July 2011; accepted 21 August 2011.

List of Abbreviations: CTL, cytotoxic T lymphocyte; HIV, human immunodeficiency virus; HLA, human leukocyte antigen; IFN-γ, gamma interferon; MHC-1, major histocompatibility complex class I; PBMC, peripheral blood mononuclear cell; SIV, simian immunodeficiency virus.

of this virus (9, 10). Indian rhesus macaques possessing the MHC-I allele Mamu-B*17 tend to show smaller viral loads after SIVmac239 challenge (11). These findings imply possible HIV control by induction of particular effective CTL responses.

The potential of Gag-specific CTL responses to contribute to viral control was suggested by a cohort study indicating association of HIV control with the breadth of Gag-specific CTL responses (12). This was supported by an *in vitro* study indicating the ability of Gag-specific CTLs to respond rapidly to SIV infection (13). We previously developed a prophylactic AIDS vaccine using a Sendai virus vector expressing SIVmac239 Gag (14) and showed that Gag-specific CTL responses were responsible for vaccine-based SIV containment in a group of Burmese rhesus macaques possessing the MHC-I haplotype *90-120-Ia* (15, 16). Furthermore, our recent study analyzing the potential of $CD8^+$ cells to suppress SIV replication *in vitro* suggested association of *in vitro* anti-SIV efficacy with numbers of Vif-specific CTL frequencies (17). We also found weaker correlation between anti-SIV efficacy and numbers of Nef-specific CTL frequencies. These results imply the potency of Gag- and Vif-specific (and possibly Nef-specific) CTLs in suppressing HIV/SIV replication.

The immunodominance patterns of these potent CTL responses could be affected by host MHC-I genotypes (18, 19). Better understanding of these MHC-I-associated CTL immunodominance patterns during primary HIV/SIV infection would contribute to elucidation of the interaction between viral replication and host CTL responses. In the present study, we examined whether Gag- and Vif-specific CTL responses are efficiently induced during primary SIVmac239 infection in three groups of Burmese rhesus macaques possessing different MHC-I haplotypes. One group did not induce Gag- or Vif-specific CTL responses, whereas the other two groups elicited Gag- and Vif-specific CTL responses efficiently. These groups of macaques would be useful for analysis of the impact of Gag- and Vif-specific CTL responses on SIV replication *in vivo*.

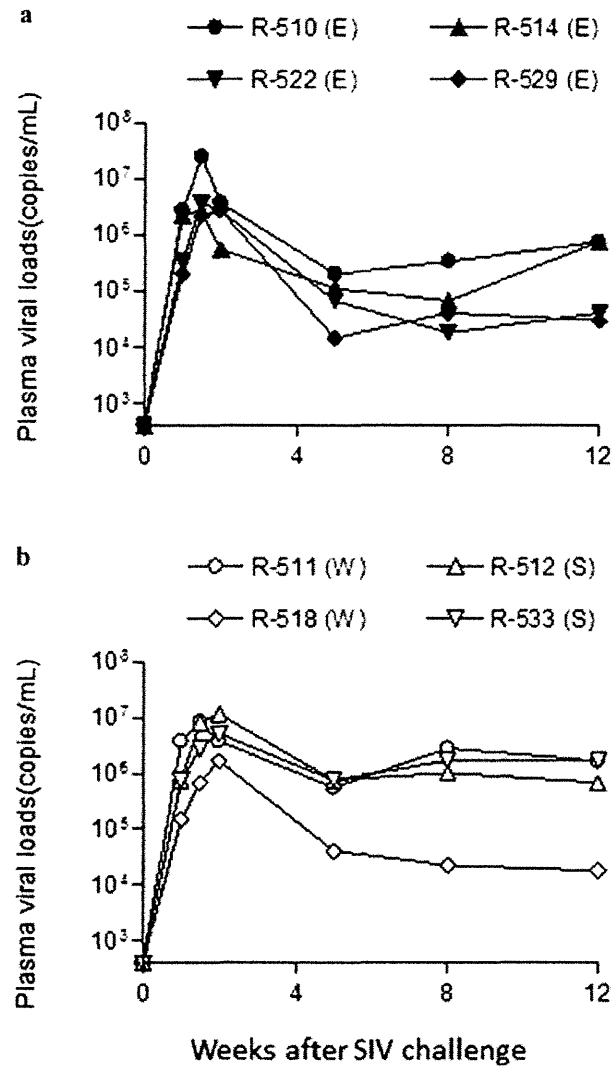

Fig. 1. Plasma viral loads after SIV challenge. (a) The first group of Burmese rhesus macaques, which possessed MHC-I haplotype *90-010-Ie* (R-510, R-514, R-522, and R-529) and (b) the second group, which possessed *89-075-Iw* (R-511 and R-518) and the third group, which possessed *91-010-Is* (R-512 and R-533) were challenged with SIVmac239. The viral loads (SIV gag RNA copies/mL) were determined as described previously (15).

MATERIALS AND METHODS

Animal experiments

Animal experiments using Burmese rhesus macaques (*Macaca mulatta*) possessing either the MHC-I haplotypes *90-010-Ie*, *89-075-Iw* or *91-010-Is* were performed in the Institute for Virus Research, Kyoto University, in accordance with the institutional regulations approved by the Committee for Experimental Use of Non-human Primates. The MHC-I haplotypes of macaques were determined as described previously (20, 21). These animals were challenged intravenously with 1000 50% tissue culture infective doses ($TCID_{50}$) of SIVmac239 (22).

Analysis of virus-specific cytotoxic T lymphocyte responses

Virus-specific $CD8^+$ T-cell frequencies were measured by flow cytometric analysis of IFN-γ induction after specific stimulation as described previously (17). PBMCs were cocultured with autologous herpesvirus papio-immortalized B-lymphoblastoid cell lines pulsed with peptide pools using panels of overlapping peptides